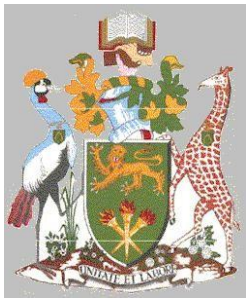

UNIVERSITY OF NAIROBI

IMPLICATION OF VOLCANO-TECTONIC AND FLUID MOVEMENTS ON SEISMIC ACTIVITY AT THE PAKA GEOTHERMAL PROSPECT IN KENYA.

BY

WANYAGA MAGDALENE WANGUI

I56/89297/2016

A Dissertation Submitted to the Department of Geology for Examination in Partial Fulfillment of the Requirements for Award of the Degree of Master of Science in Geology (Applied Geophysics) of the University of Nairobi.

DECEMBER, 2020

DECLARATION

I hereby declare that this is my original work and has not been submitted for a degree in any other university. Where other people's work, or my own work has been used, this has properly been acknowledged and referenced in accordance with the University of Nairobi's requirements

Signature: ……. Date: …….

Magdalene Wangui Wanyaga

I56/89297/2016

Department of Geology

University of Nairobi

This dissertation has been submitted for examination with our approval as the university supervisors.

Dr. Kuria Zacharia Njuguna Signature: ……. Date: …….
Department of Geology
University of Nairobi
P.O Box 30197-00100,
Nairobi, Kenya.
zkuria@uonbi.ac.ke

Dr. Mulwa Josphat Kyalo Signature: …….. Date: …….
Department of Geology,
University of Nairobi.
P.O Box 30197-00100,
Nairobi, Kenya.
jkmulwa@uonbi.ac.ke

ACKNOWLEDGEMENT

First, I thank my parents, for sponsoring me to undertake these studies and their parental guidance. My sincere gratitude goes to my supervisors Dr. Zacharia Kuria and Dr. Josphat Mulwa for their guidance and support they offered me from the beginning to the final compiling of this dissertation. I express my gratitude to Gladys Kianji, Ntuli Gift, Thomas Lecocq and the Seiscomp forum team for assisting in data processing and analysis. I would also want to thank my comrades in the seismology class for collaboration and discussions we had that made this study a success. I also highly appreciate all the people that contributed to my work in one way or another.

In particular, I thank the Almighty God for guidance, protection, grace and endurance that empowered me to cope with the academic life's challenges and saw me through the whole education process.

ABSTRACT

Seismic hydraulic diffusivity at the Paka geothermal prospect is investigated to examine the implications of fluid movements and volcano-tectonic activity on the seismic activity at the geothermal prospect. This is achieved by estimating the seismic hydraulic diffusivity from a source that originates from a point where the pore pressure propagates from for a distance (r) and time (t) from the single source that initiated the seismic swarms to each earthquake in the swarm. The seismic events located for the two years are mainly shallow seismic events that have magnitudes with a range of $0.29 \geq MLv \leq 3.62$ and at focal depths ranging from 0.8 km to 18.3km. This is due to their occurrence along the Kenyan arm of the East African Rift system where there is thinning of the crust as a result of the rifting and volcanic processes. The seismic events showed linearity with the major rift faults in the area. From the analysis of the seismic hydraulic diffusivity for the earthquake cluster located eastwards from the volcano has values that range from $7.5 * 10^{-2}$ m^2/s to 1.67 m^2/s. The regions with high seismic hydraulic diffusivity values have a high pore pressure variation in comparison with the regions with lower seismic hydraulic diffusivity values. This is as a result of the dependence of pore pressure variation on the diffusion of fluids in the rock mass which causes the geothermal reservoir induced seismicity as pore pressure diffusion plays a role of triggering seismicity and also decreases the coefficient of friction. The faults and fractures where the pore pressure diffusion takes place are the zones of high permeability that act as conduits of convective heat transfer. The upflow zones in the study area lie in the regions that have high seismic hydraulic diffusivities.

The focal mechanism solutions show that the faulting at the Paka geothermal prospect has; normal, normal strike-slip, reverse, reverse strike-slip, strike-slip reverse and strike-slip normal with nornal faulting being dominant. The strike directions from the inversion of the focal mechanism solutions are NW-SE, NE-SW and E-W strike directions on the faults; representing the regional tectonic stresses and local magmatic effects on the stresses. The tectonic regime at Paka is a normal faulting regime

TABLE OF CONTENTS

LIST OF TABLES

LIST OF FIGURES

ABBREVIATIONS, ACRONYMS AND SYMBOLS USED

D - Seismic Hydraulic Diffusivity

EARS - East African Rift System

E-W – East to West

GDC – Geothermal Development Company

GMT – Generic Mapping Tools

GUI – Graphical User Interface

L - Distance

m^2/s – meter squared per second

Ml – Local Magnitude

MLv - Local magnitude calculated on the vertical component using a correction term to fit with the standard ML

NE – North east

NNE – North North east

N-S – North to South

NW – North West

P – P wave/ Phase

RIS – Reservoir Induced Seismicity

rt – mseed – Reftek to Mini-seed

S – S wave/ Phase

SDS – Seiscomp Data Structure

SE – South East

t - Time

CHAPTER 1. INTRODUCTION

1.1. Background Information

The characterization of hydraulic properties in fluid-induced seismicity is an important and difficult task in reservoir geophysics especially in geothermal areas located in regions of active tectonic activity. Fluid induced seismicity results from injection of fluid back to a geothermal reservoir where the microseismicity is caused by the linear relaxation of the pore pressure perturbation (Serge A Shapiro et al., 2005), or from the spontaneously triggered natural microseismicity within the geothermal reservoir. The natural microseismicity in such cases present as earthquake swarms (Parotidis et al., 2003, 2005; S A Shapiro & Dinske, 2009; Serge A. Shapiro, 2000)

Earthquake swarms are characterized by many small magnitude earthquakes that do not have a main earthquake shock and are often found in volcanic and/or tectonic active areas (Sigmundsson et al., 1997) such as in the Somma-Vesuvius volcano(Saccorotti et al., 2002), and the Vogtland Seismoactive region (Parotidis et al., 2003) where many of the earthquake swarm regions are found within Quaternary volcanos(Spicak & Horalek, 2001). According to Brauer *et al.* (2003) earthquake swarms are caused by the increase in pore pressure perturbations which results from the fluid flow within the reservoir and the faults act as conduits of the fluid flow.

Seismic hydraulic diffusivity is the hydrologic property that controls the pore pressure diffusion and its estimation is a technique used to determine the pore pressure diffusion which is a triggering mechanism for earthquakes (Parotidis et al., 2005). The pore pressure diffusion is mostly responsible for the buildup of fluid pressure and the onset of seismicity (Talwani et al., 2007). It provides information on the triggering mechanism of earthquakes in a volcano-tectonic setting also

giving information on the flow direction of the pore fluids. To study the correlation between the distribution of natural seismicity and seismic activity induced by fluid transmission, a study on the microseismic activity is carried out.(Bourouis & Cornet, 2009; Serge A Shapiro et al., 2002). This correlation between seismicity and fluid movements through pore pressure diffusion in Kenyan geothermal reservoirs is carried out in the stage where fluids are injected back to the reservoir and not fully examined in the exploration stage where the seismicity is natural (Simiyu, 2000).

This study's aim is to investigate the correlation between the seismicity and fluid circulation in a reservoir induced setting in this case a geothermal system. It focuses on the Paka Geothermal Prospect in Kenya where the seismic hydraulic diffusivity of the earthquake events occurring in a cluster will be estimated. The Paka Geothermal Prospect is an interesting area for carrying out this study as it lies on the East African Rift System (EARS), it has a volcano-tectonic setting as it lies at the Paka volcano (Mutonga, 2013), there has been no fluid reinjection that has been carried out in the area thus the study relies on reservoir induced seismicity (RIS) to determine the seismic hydraulic diffusivity using the linear fluid-rock interaction(Talwani & Acree, 1985). The seismic hydraulic diffusivity (D) a function of two parameters which are the distance (r) the wave has propagated and the time (t) taken by the wave to propagate (Parotidis et al., 2005; Serge A. Shapiro, 2000; Serge A Shapiro et al., 2002);

$$r^2 = 4.\pi.D.t$$

1.2.Location of Study Area

The Paka geothermal prospect lies at the Paka volcano which is a Quaternary complex volcano with multi-vents and comprises of basalts and trachytes. It covers an area of about 280 km^2 and a height of 1697 meters above sea level and lies north of Lake Baringo. The volcano has an extensive

caldera of approximately 1.5 km and also has minor volcano centers which are linked by linear basalt and trachyte zones, and fissures to the main volcano (Mutonga, 2013). According to (Dunkley et al., 1993; Mutonga, 2013), the geothermal manifestations at the surface comprise of; geothermal grass, hot ground and fumaroles associated with hydrothermal alterations evident at the northern rims and the summit.

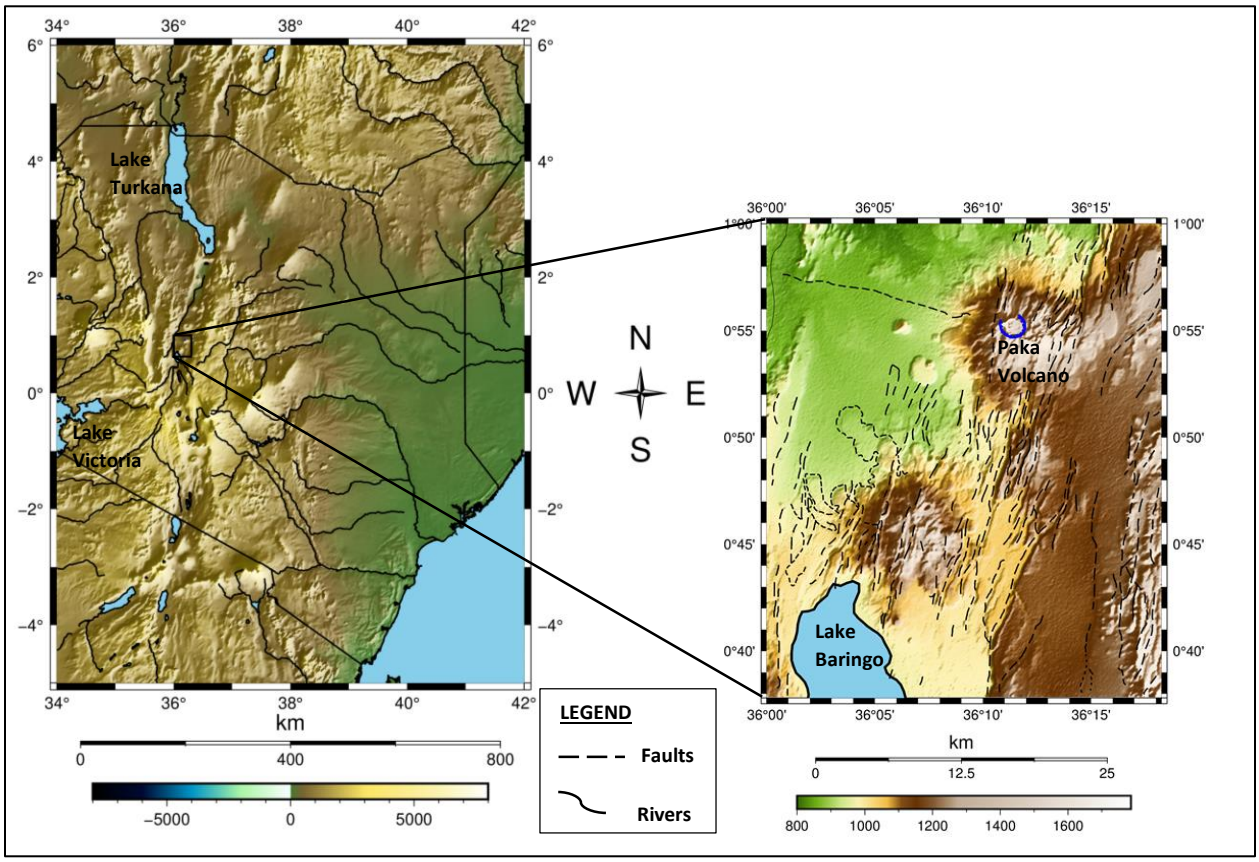

Figure 1: A map of the Paka geothermal prospect area.

1.3.Statement of the Problem

Epicentral trends determined previously from seismic monitoring in geothermal areas can be utilized to determine source properties of the seismic activity in relation to fluid flow (Simiyu & Keller, 2000). To study the correlation between the distribution of natural seismicity and seismic activity induced by fluid transmission, a study on the microseismic activity is carried out, this has

not been fully investigated in the Kenyan geothermal areas. (Bourouis & Cornet, 2009; Serge A Shapiro et al., 2002). Seismic events that occur as a result of fluid movements from previous studies have seismic phases that are not clear with well-defined onset time in comparison to earthquakes that result from the volcano-tectonic processes. Studies on pore pressure diffusion have been carried out in the exploitation stage of a geothermal field in particular during reinjection of fluid back to the geothermal system thus causing induced seismicity. However, studies on pore pressure diffusion, and its hydrologic property; the seismic hydraulic diffusivity on geothermal reservoir induced seismicity have not been carried out in the Kenyan geothermal fields.

The Paka Geothermal prospect is an ideal location to study the diffusivity of natural seismic events since fluid injection has not been done in the area and therefore the seismic activity is due to natural events. In this study, the effect that fluid flow has on seismic activity at the Paka Geothermal prospect was determined by calculating the seismic hydraulic diffusivity (D) of all seismic events with respect to each station's location and time taken for the wave-front to propagate to the station

1.4.Aim

To study the seismic hydraulic diffusivity in order to understand the correlation between fluid movements and seismic activity at the Paka geothermal system.

1.4.1. Specific Objectives

- To determine the precise hypocentral locations, outline seismic event location and correlate them with the causative faults
- To determine the focal mechanisms and establish the style of faulting and fault plane orientation.

- To estimate the seismic hydraulic diffusivity, and establish the source properties in the causative faults.

1.5. Justification and Significance of the Study

A study on the effect that fluid movements have on the seismic activity at the Paka geothermal prospect will provide an improved understanding of the geothermal prospect and other geothermal are_{as} in Kenya. The results accrue from this study are expected to contribute to the professionals working in geothermal prospecting. These includes understanding the geothermal system better before production and being used as a baseline for fluid injection stage. Additionally, it will help in delineating the regions that have high permeability therefore having high productivity. The characterization of the focal mechanisms will give an insight in the active faults orientation and their tectonics. The stress diffusion mechanism in geothermal systems, pore pressure diffusion, will be used to determine the relationship between seismicity and fluid circulation.

The determination of hypocentral locations helps to outline the locations of the seismic events as well as information on event depth and magnitude. The alignment and depth of hypocenters will be used in locating the causative faults and distinguish them from the inactive faults in the area. These causative faults will be used in identifying the locations of future earthquake by mapping the heterogenesis and asperities in the fault zones.

The determination of focal mechanisms will provide a better insight on the faulting style and orientation of fault planes. Fault plane solutions can be distinguished from regional tectonics or magmatic effects on crustal stresses by studying their distribution.

Seismic hydraulic diffusivity estimation will be used to relate the spatial occurrence of seismicity and fluid flow. This results from the diffusion of pore pressure which acts as a stress transmission

mechanism in geothermal reservoirs. This is applied with the assumption that the epicentral trend increase of earthquake swarms in the study area is a direct result of pore pressure diffusion. Seismic hydraulic diffusivity provides an understanding of the source properties in the causative faults by determining the pore pressure diffusion which is used in localizing high permeability zones that act as conduits of convective heat transfer. High fluid producing wells target areas lies in these zones as they are known to have the major mass output

This study will provide a better understanding of how geothermal reservoir induced seismicity (RIS) can be used to determine pore pressure diffusion thus understand the permeability of geothermal systems as well as active seismic zones. Consequently, seismic hydraulic diffusivity can be used as a tool in determining source properties in a volcano-tectonic region, which is resourceful information to policy makers.

CHAPTER 2. LITERATURE REVIEW

2.1. Tectonic Setting and Geology

The East African Rift System (EARS) is a continental rift zone that is active, it starts from the Afar triangle to Mozambique and it begun developing in Oligocene. Paka Geothermal Prospect lies on the Eastern arm of the EARS in northern Kenyan rift. Along the axis of the Great Rift Valley, the development of shield volcanoes is evident. The rift axis is the focus in which most geothermal prospects are located which results from raised heat flow from the upper mantle, a source of the thermal bulge in the central Kenya region. The existence of low to high geothermal systems are as a result of the fracture networks resulting from the formation of the rift (Dunkley et al., 1993; Mutonga, 2013; Simiyu, 2010b; Simiyu & Keller, 2000). Volcanoes present in the Kenyan rift are inclusive of the following; Olkaria, Suswa, Menengai, Paka, Emuruangogolak, Barrier Complex, Silali, Longonot, Eburru and Korosi.

The evolution of the Paka volcano resulted from a lava shield formation that had a diameter of approximately 25 km and on the western side the formation of a tuff cone and there after the caldera's formation followed (Mutonga, 2013). There are two occurrences of trachytic eruptions that are separated by basaltic eruptions and faulting. The geological sequence of the area consists of the Lower trachytes, Lower basalts, Upper trachytes, pyroclastic deposits and trachyte and mugearite an oligoclase basalt. The eruption of the lower basalts occurred from fissures located on the eastern margins of the volcano and faulting which formed the NNE trending faults accompanied this eruption. The axial zone evident on the eastern and western margins of the volcano resulted from repetitive faulting. The caldera was formed as a result of the pyroclastic activity that caused the summit to collapse. Normal faulting dominates the study area with N-S trending faults on the southern flanks and a deviation to the NNE direction towards the summit

and NE direction on the western boundary faults and on the eastern flanks. There is an evident NW-SE elongation of the volcano which resulted from regional stresses (Dunkley et al., 1993; Hackman, 1988; Mutonga, 2013).

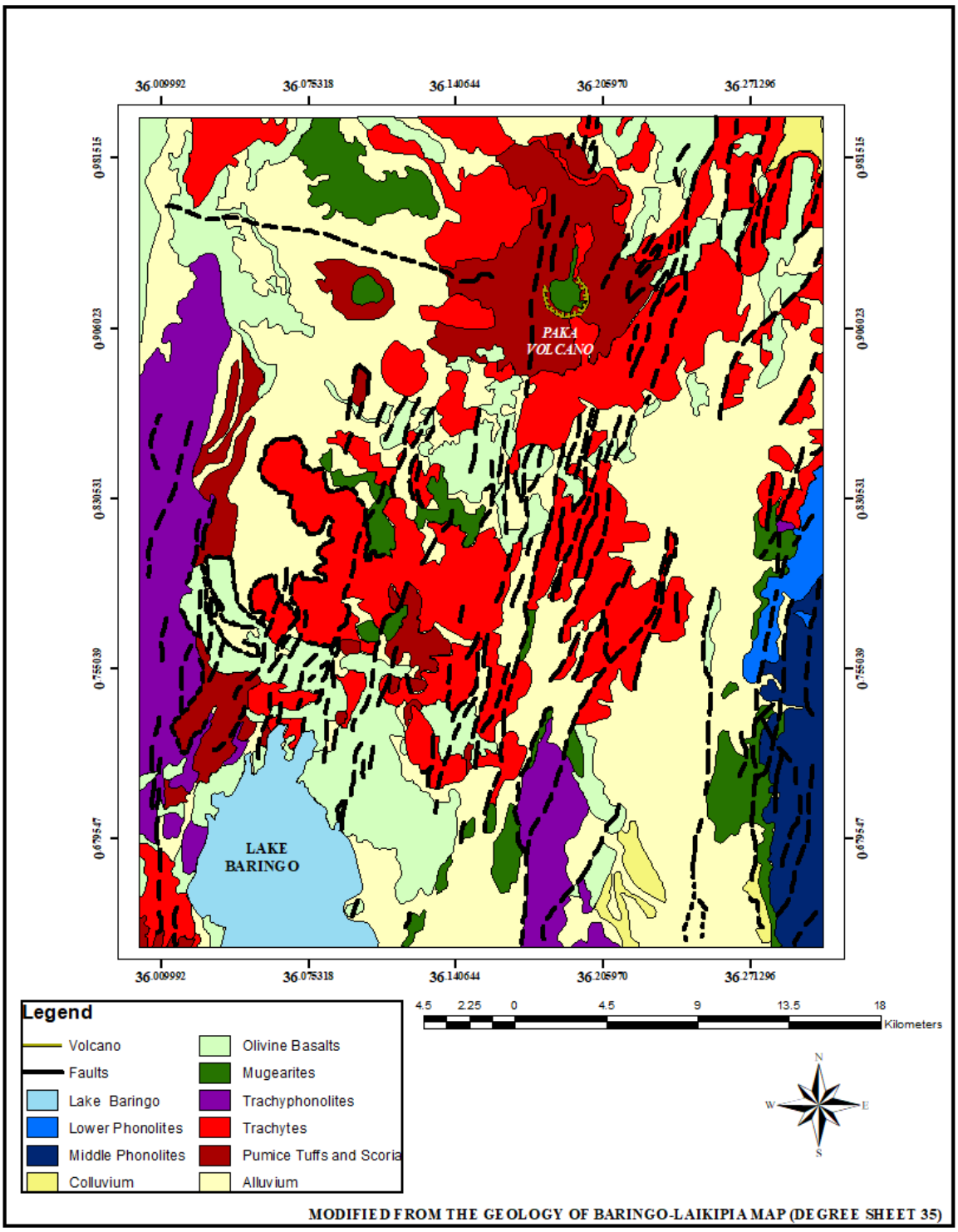

Figure 2: The geology of the Paka Geothermal Prospect Area modified from the Geology of Baringo-Laikipia map (Degree Sheet 35) (Hackman, 1988).

2.2. Geothermal Background

In 2006-2007 a comprehensive geothermal potential study was carried out at the Paka area. The manifestation of the geothermal system at the Paka area is widespread through the evidence of hot grounds, fumarolic activity, rocks altered by the hydrothermal activity and sulfur deposits. The results from the study show that a heat source that is centered at depth below the summit crater and extending towards the east drives the geothermal system at Paka. The syenitic nodules present within the pyroclastic deposits that which erupted as the caldera was formed show the evidence of a magmatic body that is shallow. The possible geothermal heat source is a trachyte or a trachyte-basaltic body that underlies the volcano. There is evidence of deep seated faults from fumaroles that have sulphur deposits that are well-crystalized on the Eastern crater. The permeability of the geothermal reservoir is mainly controlled by a wide graben that runs in the NNE direction across the volcano massif. From chemical geothermometry analysis, the estimated temperatures at the reservoir are between 180°C and 300°C and the estimated potential is above 500MWe (Simiyu, 2010b). According to Dunkley et al, (1993) (figure 3), there are seven areas in which the geothermal activity is located at Paka. These include:

- Eastern crater: The areas with the maximum activity have temperatures between 90°C and 95.9°C and those with the minimum activity having temperatures between 40°C and 80°C. There exists a large fumarole producing a visible steam plume on the eastern edge of the crater.
- Old crater and Western margins: The activity is evident in the linear zone trending in NNE direction alongside the western boundary fault. The fumarolic activity is weak with temperatures between 48.7°C and 77.5°C.

- Caldera: There is extensive activity with the basaltic scoria cone having the largest intensity. There are several fumaroles that have temperatures above 80°C. It lies in the fault zone trending northwards.
- Southern margins: On the pyroclastic deposits there are weak fumaroles with temperatures of 42.7°C to 77.5°C.
- Northwestern flanks: The activity lies on an extensive zone on the fault that trends in the NNE direction on the western margin, the temperature exceeds 90°C. The activity is intense in three zones as shown below;
    - Zone A; It has temperatures of up to 96.1°C and lies between two parallel faults trending northwards.
    - Zone B; Lies on the upper margins of the volcano and trends in the NNE direction with temperature between 46.7°C and 93°C.
    - Zone C; It lies on discrete fault-controlled areas having temperature between 35.5°C and 96.3°C. It has a general trend in the NNE direction.
- Murulen: The geothermal activity is isolated and lies on the basaltic scoria cone with the temperature reaching a high of 39.9°C.

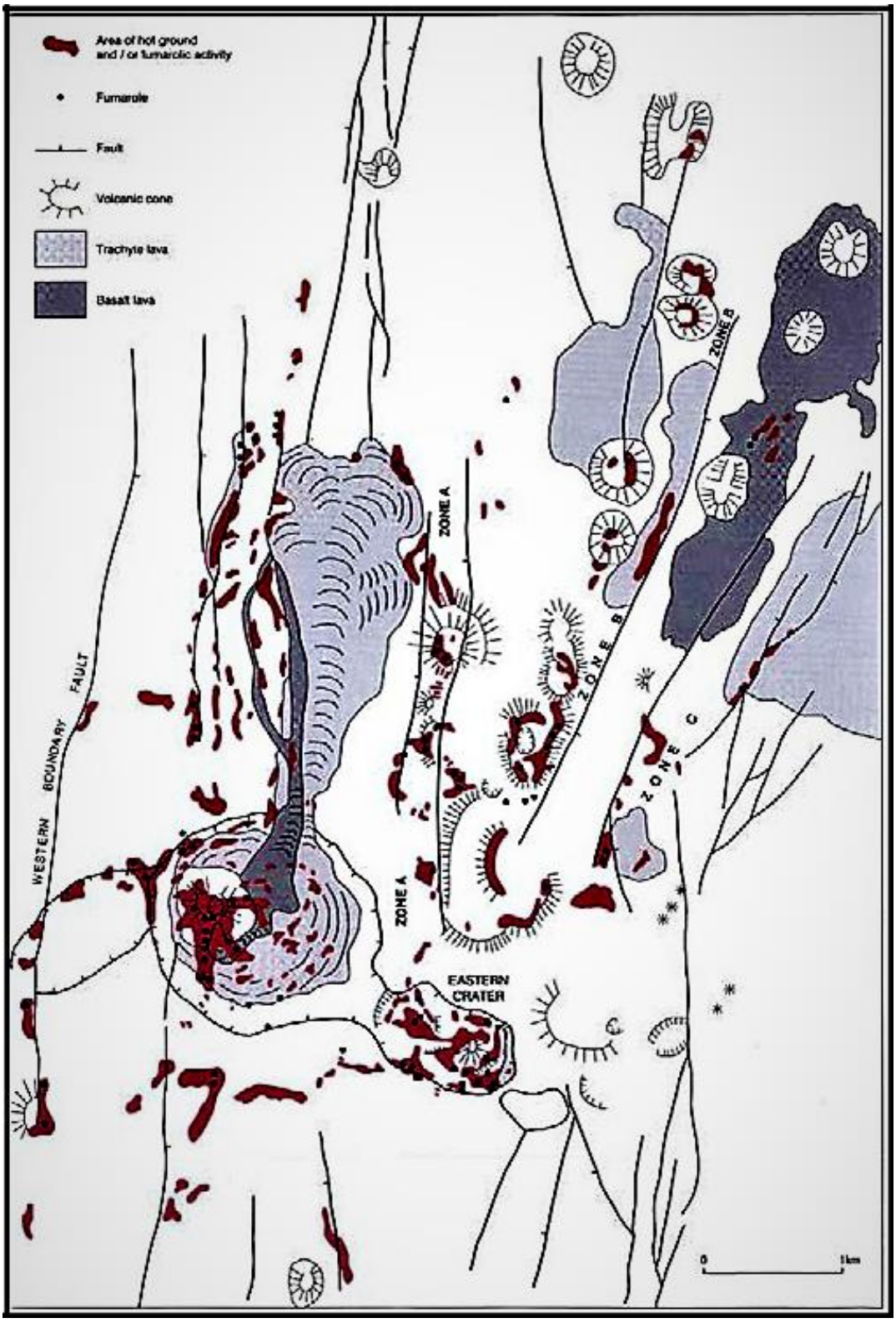

Figure 3: The active thermal areas at the Paka area and their association to the faults (Dunkley et al. 1993).

2.3.Seismicity

Beneath the eastern part Paka volcano, seismicity exhibits a pipe-like outline which has an anomalous low velocity of the S phase due to the an active fluid flow signifying geothermal potential at depths of 3 km to 6 km. The Paka area is characterized by significantly low magnitude (ML<3) background seismicity which outlines both the NE-SW striking structures. The Focal mechanisms show the P-axis striking in the NE-SW direction and indicate that the faulting is controlled by local stresses as well as tectonic regional stress. Beneath the volcano there are seismic events that have small magnitudes and are shallow, they result from the weaker upper crust where the earthquakes are associated with lower depths in the crust in the magmatic sections of the rift where there is a possibility of magmatic fluids exsolving slowly (Patlan et al., 2017; Simiyu & Keller, 2000).

There are two key layers of the crust in the Paka area from studies on the velocity structure by (Kangogo et al., 2018), the first one is 10 km thick with a P-wave velocity between 2.63 km/s and 5.94 km/s, the second one is 12km thick with a P-wave velocity between 5.94km/s and 7.08km/s. The second layers lower velocity boundary corresponds to the Moho discontinuity that is sharp. The velocity of the S wave in the crust id 3.75km/s.

From a passive seismic study on the seismic activity in the northern area of the Kenyan Rift Valley (KRISP 81) by (Pointing et al., 1985) carried out in the first months of 1981, seismic events with north-south linearity were located within the Rift which ran from Suguta valley in the north and Lake Baringo and Bogoria in the South. In Lake Turkana's southern area, the seismicity was more diffuse. Around the northern part of Kenya where a there exists a broad zone of splay faulting, there was slight seismic activity. The activity within the Rift was separated by a relatively quiet zone from a second, north-south, diffuse zone located further eastwards (Pointing et al., 1985).

According to a study done by (Henry et al., 1990) on the seismicity of the Kenyan rift valley under the (KRISP 85) study where two seismic profiles; alongside the axis and across it were used to investigate the structure of the crust using the long-range explosion seismology, there is an occurrence of a moderate crustal thinning in the central segment of the rift.

In January 1990 to March 1990 a temporary seismic network was set up in the Lake Baringo basin, which was used to investigate the earthquake occurrence by (Tongue et al., 1994). The results from the study showed a location of eighty local earthquakes within the central rift with magnitudes less than two, at a depth of 5 km beneath Lake Baringo, there was evidence of earthquake swarm activity. The earthquakes showed an association with the main rift faults, there was also a brittle-ductile zone if transition at 12 km to 16 km depths. There is a WNW-ESE extension and stress regime from the focal mechanisms and shear wave polarizations analysis.

According to the seismic studies carried out in the study area as well as in the Kenyan rift show that there is crustal thinning in the rift especially in the volcanic centers, there earthquakes that occur are mainly small magnitude and shallow due to the existence of a weak upper crust and the stress regime from focal mechanism solutions is controlled by both the regional stress as well as local magmatic stresses. However the study on the fluid movement association with the natural seismicity in the geothermal reservoirs has not been carried out.

CHAPTER 3. MATERIALS AND METHODS

3.1. Introduction

There are several seismic stations installed at the Paka Volcano operated by the Geothermal Development Company. The seismic network was installed in 2009 to monitor the seismic activity at the area as well as investigate the geothermal potential of the prospect. The stations are equipped with Guralp CMG-40T seismic sensors and Reftek 130 dataloggers. The data for this study was obtained for a two year period where a total of 100 seismic events were recorded for the Paka Geothermal Prospect area.

3.2. Software Used in Seismic Data Analysis

The operating system used for this study is Ubuntu 16.04.

SEISCOMP3- This is a software package that is used in acquiring seismic data and exchange of the data in real time through Seedlink. It has capabilities to carry out processing of the data automatically. The graphical user interfaces (GUIs) are used for visualization, quality control and in reviewing the events. Spread is used as a communication tool between the different modules in the software, it is based on TCP/IP infrastructure. The package consists of three main components; Data acquisition using SeedLink and ArcLink; Data Processing which used various modules such as Scautopick to automatically process the data and the Graphical User Interfaces which are used to display and also as post-processing tools such as Scolv (Saul et al., 2015; *SeisComP3 Seattle Documentation*, 2013).

Generic Mapping Tools (GMT) - this is an open-source software that contains command line tools and map projections. It uses Cartesian and geographic data where processes such as gridding, trend fitting, filtering and projecting are carried out and the output produced in the Post Script format

which ranges from 3D views, contours maps, x-y plots to artificially illuminated surfaces (*The Generic Mapping Tools Documentation*, 2019).

STRESSINVERSE- this is a Python or MatLab software package that uses focal mechanisms to carryout inversion for fault orientations and stress (Vavryčuk, 2014).

FMC- this is a software uses focal mechanism data to compute the various parameters of earthquakes, then classifies the rupture type, it also performs cluster analysis of the data (Álvarez-Gómez, 2019)

SURFER – this is used in visualization and analysis of data sets.

ARCGIS – this was used in geoereferencing, digitizing and the generation of maps.

Microsoft Excel – it was used in performing calculations.

3.3.Methods

The first part of data processing was done in Seiscomp3. This included archiving the data in the Seiscomp Data Structure, locating the seismic events automatically, revising the origin information, relocation of the seismic events and determining the fault plane solutions using the P- phase polarity first motion method. The location of seismic events in Seiscomp3 was carried out in offline mode without connecting to the messaging nor to the database because the data was not real-time using playback modules in the Ubuntu Terminal. The second part was carried out using the following software; STRESSINVERSE carry out an inversion of the focal mechanisms, FMC to compute the seismic event parameters and of estimating the seismic hydraulic diffusivity was carried out in Microsoft excel.

3.3.1. Pre-Processing and Data Preparation

The data acquired was in the raw Reftek format. First, the data was rearranged from hourly data to daily data, then converted into Mini-seed format, this was done using a Reftek to-mini-seed script which used the rt-mseed package ran in the Ubuntu terminal (*REF TEK Utilities Users Guide*, 2006).

3.3.2. Initial processing

The mini-seed format data was then loaded into Seiscomp3 using the Seiscomp Data Structure (SDS) by rearranging the data according to the stations and channels which was stored into an archive folder ~/seiscomp3var/lib/archive. It was then Scarted by creating playback files which are multiplexed mini-seed files from the data in the Seiscomp Data Structure (SDS) archive in offline mode, the output was stored in an xml file instead of in the database using scart an archive tool used to import or export Mini-seed data to and from an SDS archive After scarting the data a search of waveform anomalies in the form of changes in amplitudes was done using the Scautopick module which uses the third-order Butterworth filter with corner frequencies of 0.7Hz and 2Hz. Scautopick also calculated the amplitudes for the given magnitude types where the window started at the P-phase pick time, the P-phase picks were then stored in an xml file.

Scautoloc module was then used to locate the events automatically using the P-phase picks file created by scautopick by reading the P-phase picks in the file and associating them with the associated amplitudes creating an origin of the events, the output file created was an origins file stored in an xml file. At least four stations were used to locate the events, a minimum amplitude of 10 and minimum Signal to Noise Ratio (snr) of 7 was used. The xxl feature; a feature in Seiscomp3 Scautoloc module that allows creating preliminary origins with already 4 phases and amplitudes with exceptional large amplitudes area(*SeisComP3 Seattle Documentation*, 2013), was

used to allow the software to locate events in a small area and also allowed location using a minimum of four stations. The locator used was LOCSAT using an IASP91 velocity profile for the initial automatic location.

The scamp module was then used to calculate the amplitudes based on the origins and picks associated with them. The input file is the origins file created by scautoloc and an output file origins-with-amps is created.

The next step was calculating the magnitudes from the amplitudes where the scmag module was used. This module does not access the waveforms. The purpose of scmag is the decoupling of magnitude computation from amplitude measurements. The local magnitude MLv was calculated on the vertical component. The input file was the origins-with-amps file and the output file origins-with mags file.

Finally, the event was determined using the scevent module which associated the origins to an event by using matching P-phase picks. The input file is the origins-with-mags file and the output file is the events file that holds all the events.

Since the analysis was all done in the offline mode, the information was then populated into the database using the scdb utility in Seiscomp3 (*SeisComP3 Seattle Documentation*, 2013)..

3.3.3. Post Processing

The results in Seiscomp3 were saved as an xml document which was viewed using the graphical interface module scolv. The seismic events were listed in the events tab which showed the event The dominant strike direction in the study area is the E-W direction. These focal mechanism solutions represent the regional tectonic stresses and local magmatic effects on the stresses.

Information such as event ID, event time, magnitudes, location and depth (*SeisComP3 Seattle Documentation*, 2013) as shown in the figure below;

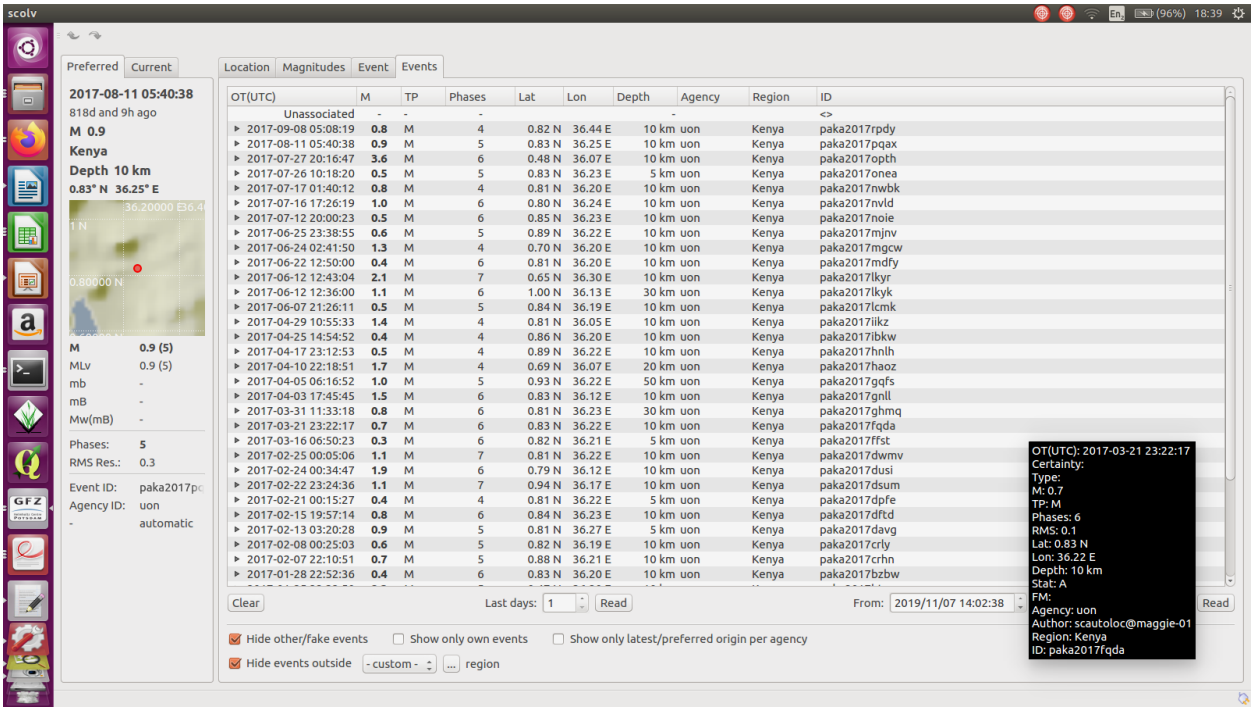

Figure 4: Events catalogue in the scolv module.

The scolv Graphical User Interface was used to review the origin information such as picks, location, depth, time, magnitudes, and event association. The origin information in the events file was loaded into scolv. The first process was carrying out the waveform review using the waveform picker window. The process of waveform review was as follows (*SeisComP3 Seattle Documentation*, 2013):

1. Select an event from the events tab.
2. Click on Picker which opens the waveform picker window.
3. Select a waveform trace from the trace list containing traces for each station.
4. Zoom the trace and repick the P-wave.

5. Define the Pick Polarity, this can either be *positive*, *negative*, *undecidable*, or *unset*. If set it is displayed as an arrow.
6. Accept the picked phase
7. Repeat steps 3, 4, 5 and 6 for all traces
8. Apply the changed picks to the origin and update the residuals which closes the waveform picker window
9. Relocate using LOCSAT and the Paka velocity model profile
10. Compute magnitudes
11. Confirm the event
12. Change to the events tab
13. Go to 1

The scrtdd module in Seiscomp3 was used in the relocation of the seismic events using the Double Difference relocation method by applying the Least Squares algorithms LSQR (Paige and Saunders, 1982) and the LSMR algorithm (Fong and Saunders, 2011), a velocity model for the Paka area was used in the relocation. An event catalogue was generated for the relocation process where three files were extracted from the seiscomp3 database, they included the Event.csv, Phase.csv and Station.csv files. The event file contained the following event information; the event Id, latitude, longitude, date and time, depth, magnitude and rms (root-mean-square); the phase file contained information on the phases used and the station file contained information of the seismic stations used in such as the location Id, latitude longitude, depth and seismic network..

After the relocation was done three files were generated; the reloc-event.csv file, reloc-phase.csv file and the reloc-station.csv file. The files were combined and converted to a seiscomp3 xml file

and loaded back to the seiscomp3 database to determine the focal mechanism solutions using the polarity of the P-wave First Motion.

3.3.4. Focal Mechanisms

The focal mechanism analysis was done in scolv graphical user interface in seiscomp3. The following process was used:

1. Select an event from the events tab.
2. Click on Picker which opens the waveform picker window.
3. Select a waveform trace from the trace list containing traces for each station.
4. Define the Pick Polarity, this can either be *positive*, *negative*, *undecidable*, or *unset*. If set it is displayed as an arrow.
5. Accept the picked phase
6. Repeat steps 3, 4, and 5 for all traces
7. Apply the changed picks to the origin and update the residuals which closes the waveform picker window.
8. Click on the first motion tab and plot the fault plane solution using the polarity of the P-wave First motion.
9. Commit the fault plane solution.
10. Change to the events tab
11. Go to 1

The focal mechanisms were determined using the first motion of P- wave polarities where the first motion detected at a particular station was either motion up for compression (push away) from the focus, motion down for dilatation towards the focus or undecidable where there was no apparent signal (Cronin, 2010) as shown in figure 6 below;

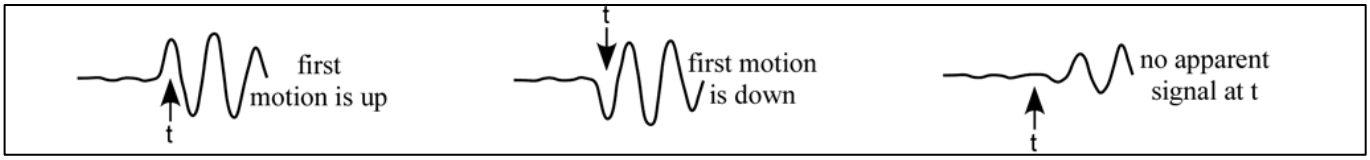

Figure 4: Compression and Dilatation of first motion (Cronin, 2010)**.**

The P-wave travels to the seismograph from the earthquake hypocenter on a curved path due to the variation of the seismic velocities with varying depth and different mediums. For every single ray, the calculation of the takeoff angle which is the emergence angle, the azimuth from the hypocenter to the seismograph and a vertical imaginary line that extends through the hypocenter is done

Polarities were set as either positive for motion up, negative for motion down, or undecidable where the signal was not clear. They were plotted by a solid green dot for the positive polarity, an open dot for negative polarity and an **x** for undecidable in Seiscomp3 as shown in figure 7 below;

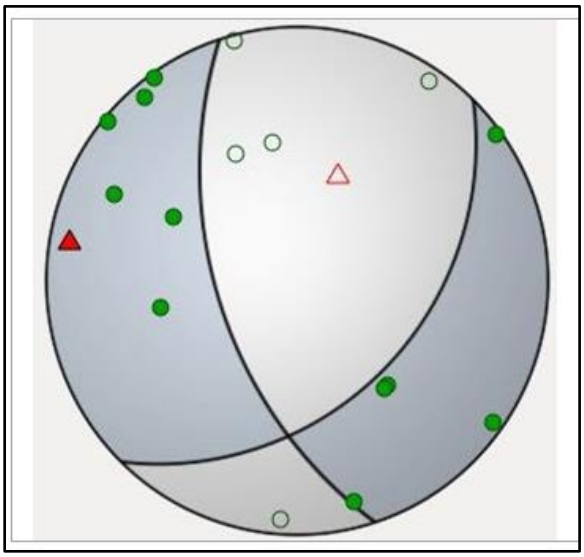

Figure 5: Focal mechanism solution using Seiscomp3 showing first motion up (green dot) and first motion down (open dot) (Sira et al., 2014)**.**

The plot for each symbol is defined by the azimuth where it is positioned in a line that extends towards the azimuth from the center showing relativity to the hypocenter and takeoff angle. The

focal mechanism was then graphically determined by finding the best fit of the nodal planes which are two great circle arcs, the solution obtained is useful in understanding the fault type and the causative fault's orientation.

Stress inversion was carried out on the focal mechanism solutions in order to determine the faults orientation and the stress regime in the study area, this was done using the STRESSINVERSE software (Vavryčuk, 2014), an iterative joint inversion algorithm. The apart from the orientation and stress regime, the algorithm also determined two principal focal mechanisms and the focal mechanism solutions having the correctly selected fault planes.

Later FMC software (Álvarez-Gómez, 2019), was used on the focal mechanism solutions to compute the rupture type, and classification of each focal mechanism.

Both algorithms used in STRESSINVERSE and FMC were run on python.

3.3.5. Seismic Hydraulic Diffusivity

In a porous medium, the rock mass deformation and fluid flow in the pore spaces, interaction is referred to as poroelasticity. Equations by Biot (Boit, 1962), define the theory of poroelasticity in a time-dependent interaction of the fluid flow and rock mass deformation. According to the equations, there is the presence of one shear wave and two compressional waves in a system in the general case, in the presence of fluids in the system, the shear wave is neglected. The P and S seismic waves form the first compressional and shear wave propagating in the medium, the second compressional wave is defined for lower frequencies than the Biot critical frequency and is a diffusional wave. The Biot critical frequency is defined as the highest frequency where the solid-fluid friction controls the propagation of the wave which is analogous to the pore pressure diffusion (Andreassen & Fabricius, 2010; Boit, 1962; S. A. Shapiro et al., 1997). For pore pressure p,

equation of inhomogeneous diffusion is one of linear poroelasticity governing equations as shown in equation (a):

$$\frac{B}{3}.\frac{\partial\sigma_{kk}}{\partial t}+\frac{\partial p}{\partial t}=\frac{k}{\mu.S_\sigma}.\nabla^2\text{p} \dots\dots\dots\dots\dots\dots\dots\dots\dots\dots\dots\dots\dots\dots\dots\dots\dots\dots\dots\dots\dots\dots\dots \text{(a)}$$

B is the Skempton's Coefficient,

$\sigma_{kk} = \sigma_{11} + \sigma_{22} + \sigma_{33}$, the mean stress,

k is the permeability,

μ is the viscosity of the fluid,

S_σ is the coefficient of unconstrained specific storage,   and

t is the time (Parotidis et al., 2003; Wang, 2000).

In the case of fluid injections, a displacement field that is irrotational in a domain that is unbounded is assumed to be valid, as equation (i) is mathematically uncoupled from the mechanical equilibrium equations in one out of four cases, Equation (a) becomes:

$$\frac{\partial p}{\partial t}=D.\nabla^{2p} \dots\dots\dots\dots\dots\dots\dots\dots\dots\dots\dots\dots\dots\dots\dots\dots\dots\dots\dots\dots\dots\dots\dots\dots\dots\dots\dots\dots\dots\dots..(b)$$

Where D is the hydraulic diffusivity.

According to (Scholz, 2002), the earth's crust diffusivity is assumed to being between 0.01 m^2/s and 10 m^2/s. With regard to hydraulic and elastic properties, the medium in equation (b) is considered to be isotopic and homogeneous.

$$D=\frac{k}{\mu S} \dots\dots\dots\dots\dots\dots\dots\dots\dots\dots\dots\dots\dots\dots\dots\dots\dots\dots\dots\dots\dots\dots\dots\dots\dots\dots\dots\dots\dots\dots\dots.(c)$$

Equation (c) describes the relationship between diffusivity and permeability where;

S is the coefficient of uniaxial specific storage.

A solution for equation (b) was determined for a source originating from a point in a medium that is poroelastic, isotropic, saturated and homogenous and the distance r in which the pore-pressure front propagated from the source is defined as:

$$r^2 = 4.\pi.D.t \ldots\ldots\ldots\ldots\ldots\ldots\ldots\ldots\ldots\ldots\ldots\ldots\ldots\ldots\ldots\ldots\ldots\ldots\ldots\ldots\ldots\ldots\ldots\ldots\ldots\ldots\ldots\ldots\ldots\ldots\ldots (d)$$

Equation (d), is used to study the earthquake swarms initiated by pore pressure diffusion, it has been applied in various areas such as seismicity in volcanic regions (Parotidis et al., 2005; Saccorotti et al., 2002).

Studies on earthquake swarms, which are seismic sequences without a mainshock, and therefore, they have no dominant magnitude are used to study seismic hydraulic diffusivity. The earthquake swarm occur often in volcanic and/or tectonic active regions (Sigmundsson et al., 1997). It is assumed that for each earthquake swarm there is an injection point which is considered to be secondary sources that result from a single source that initiated the seismic swarms. The following criteria are defined for detection of an earthquake swarm:

- Spatial- where all seismic events in an earthquake swarm must lie within a defined volume.
- Temporal- where all seismic events in an earthquake swarm must be within a defined window of time. The starting time is defined by the first event which is assumed as the injection or the secondary source of the pore pressure perturbation (Parotidis et al., 2005; Saccorotti et al., 2002).

The seismic hydraulic diffusivity was calculated using equation (d), where (r) is the distance the waveform has propagated and (t) is the time taken for the waveform to propagate the distance. The diffusivity was calculated for an earthquake cluster that is located slightly to the east of the Paka volcano, where one event was assumed to be the initial earthquake and the other occurred as a result of fluid flow through the region the earthquakes clustered (Parotidis et al., 2005). The distance (r) is the difference between each event location and the initial earthquake location and the time (t) is the difference between the initial earthquake origin time and earthquake event time for each event in the earthquake cluster. The calculation of the seismic hydraulic diffusivity was done in Microsoft Excel with the assumption that the source of the earthquake cluster in the study area results from a single point,

The earthquake cluster is concentrated between latitudes 0.84°N and 0.91°N and longitudes 36.19°E and 36.25°E covering a volume of 7.9*10.2*16.9 km^3 in the (N-S*E-W*depth)

CHAPTER 4. RESULTS AND DISCUSSIONS

4.1. Hypocentral Locations

A total of 100 microseismic events were obtained for the Paka Geothermal Prospect area. The magnitudes have a range of $0.29 \geq MLv \leq 3.62$ and at focal depths range from 0.8 km to 18.3km. For the two-year period, most of the seismic events occur on the Eastern to Southern eastern area of the Paka volcano mostly along the highly faulted area with a few occurring north of the Paka Volcano and North of Lake Baringo. The seismic events show a NE-SW occurrence trend. Most of the events show linearity with the major rift faults (figure 7) occurring on the NNE trending faults on the eastern margins that were formed during the eruption of the lower basalts (figure 8).

The teleseismic events recorded were filtered out by the Butterworth filter with corner frequencies of 0.7Hz and 2Hz as they were not part of the objectives of the study. Beneath the volcano and south of the volcano, the seismic events have moderate depths of between 5.5 km to 8.5 km, the North eastern and eastern parts of the study area show depths ranging from 0.8 km to 5.5 km and the south west and north of the Paka volcano has depths ranging from 6km to 18 km as shown in figure 6 below:

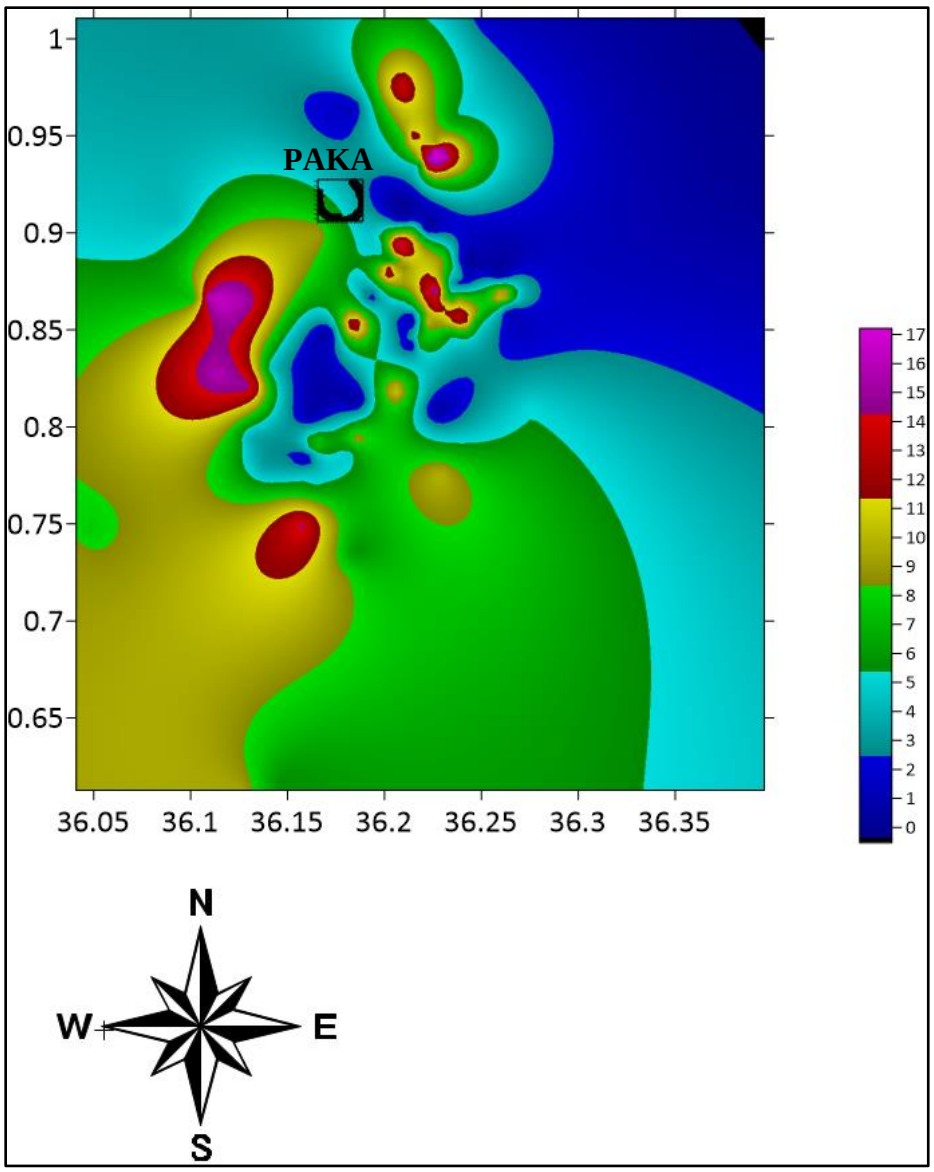

Figure 6: Depth distribution of the seismic events at the Paka geothermal prospect area.

The magnitudes at the study area are generally small magnitudes, Most of the seismic events have magnitudes ranging from $0.3 \leq MLv \leq 1.5$, and they lie on the eastern side of the volcano running from the north of the volcano to the south east of Paka volcano. A few seismic events have magnitudes $MLv \geq 1.5$ most of which lie north of Lake Baringo. There are two events that have $MLv \geq 3$ which are located east of Lake Baringo as shown in figure 7.

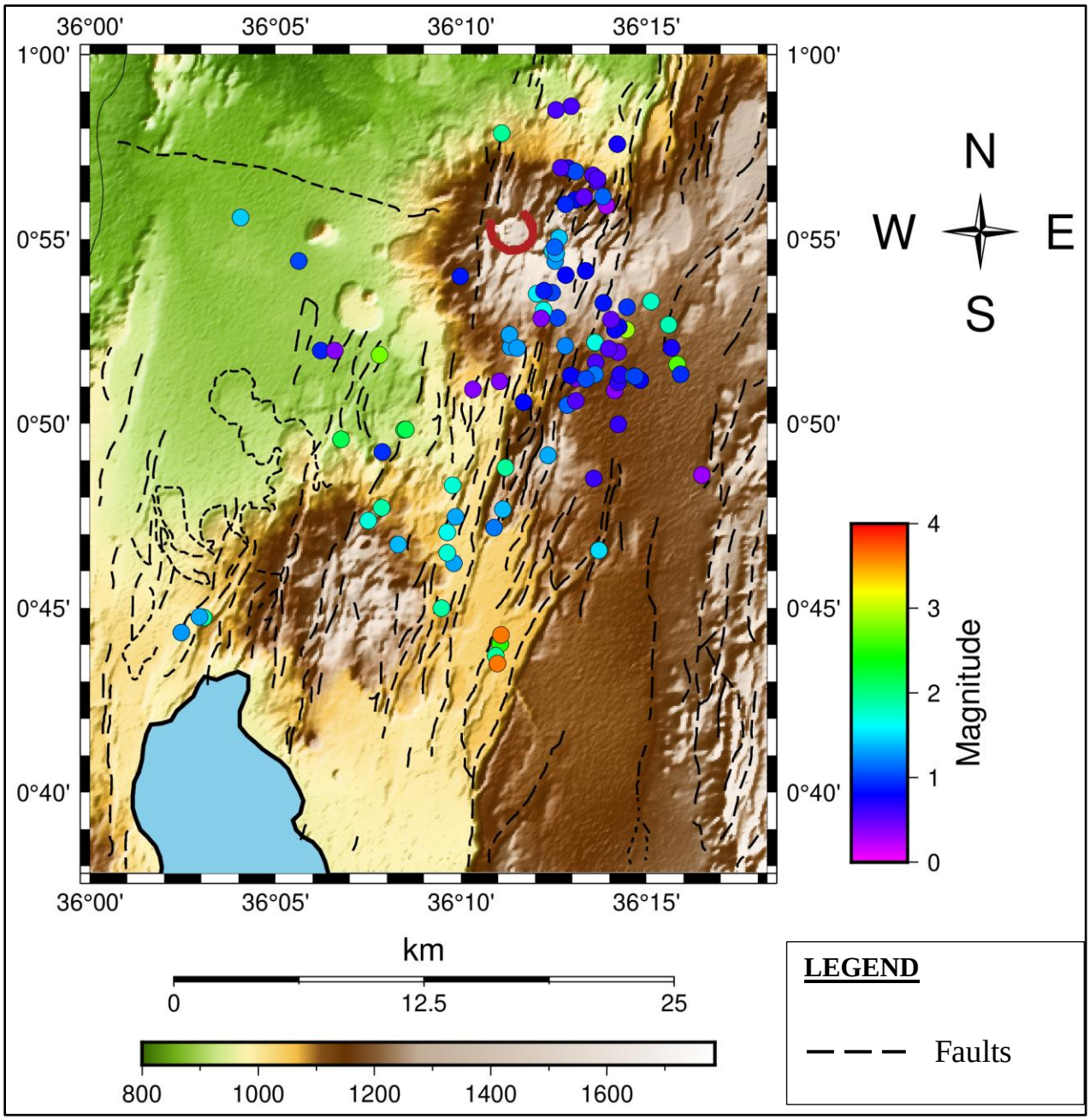

Figure 7: Seismic events at the Paka geothermal prospect showing the varying magnitudes.

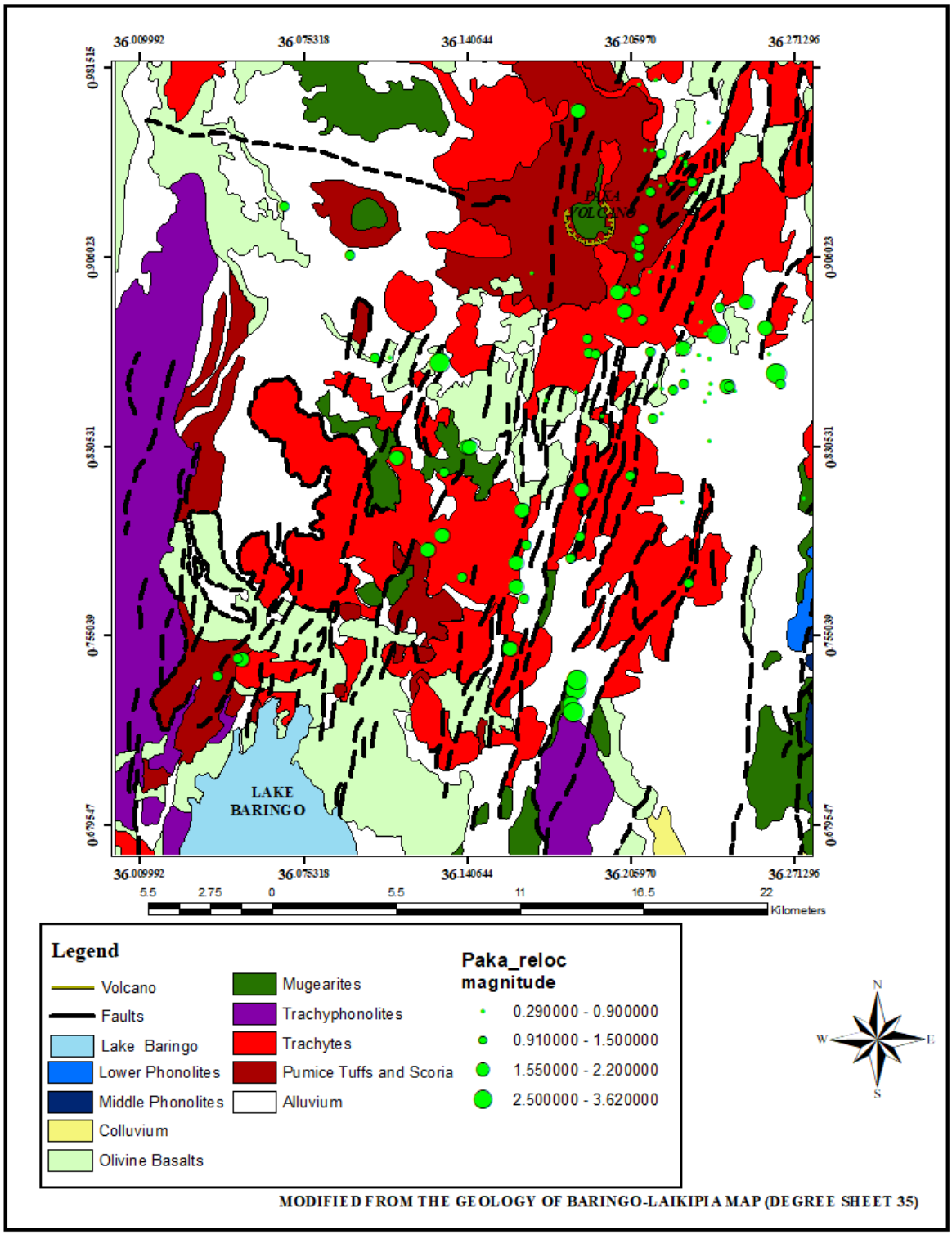

Figure 8: Earthquake hypocenters at the Paka Geothermal Prospect showing the their geology and faults .

4.2.Focal Mechanisms Solutions

The focal mechanisms were determined using the graphic technique from first-motion P-wave polarities. 31 seismic events were used in the determination of the focal mechanisms from the relocated events. Normal and normal strike-slip faulting are the dominant faults type in the area, the other fault types present are; reverse, reverse strike-slip, strike-slip reverse and strike-slip normal. Figure 9 below shows the faults classifications computed from the focal mechanisms solutions of the Paka geothermal prospect. Figure 10 shows the graphical representation of the focal mechanisms. The focal mechanisms of the corrected fault planes from the inversion of stress show that the strike direction in in the NW-SE, NE-SW and E-W directions.

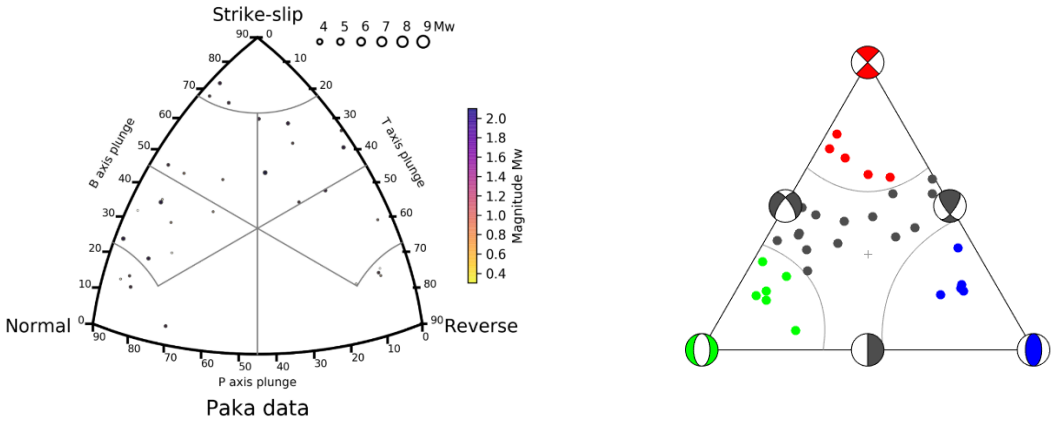

Figure 9: Faults classification from the focal mechanisms at the Paka area showing dominant normal faulting.

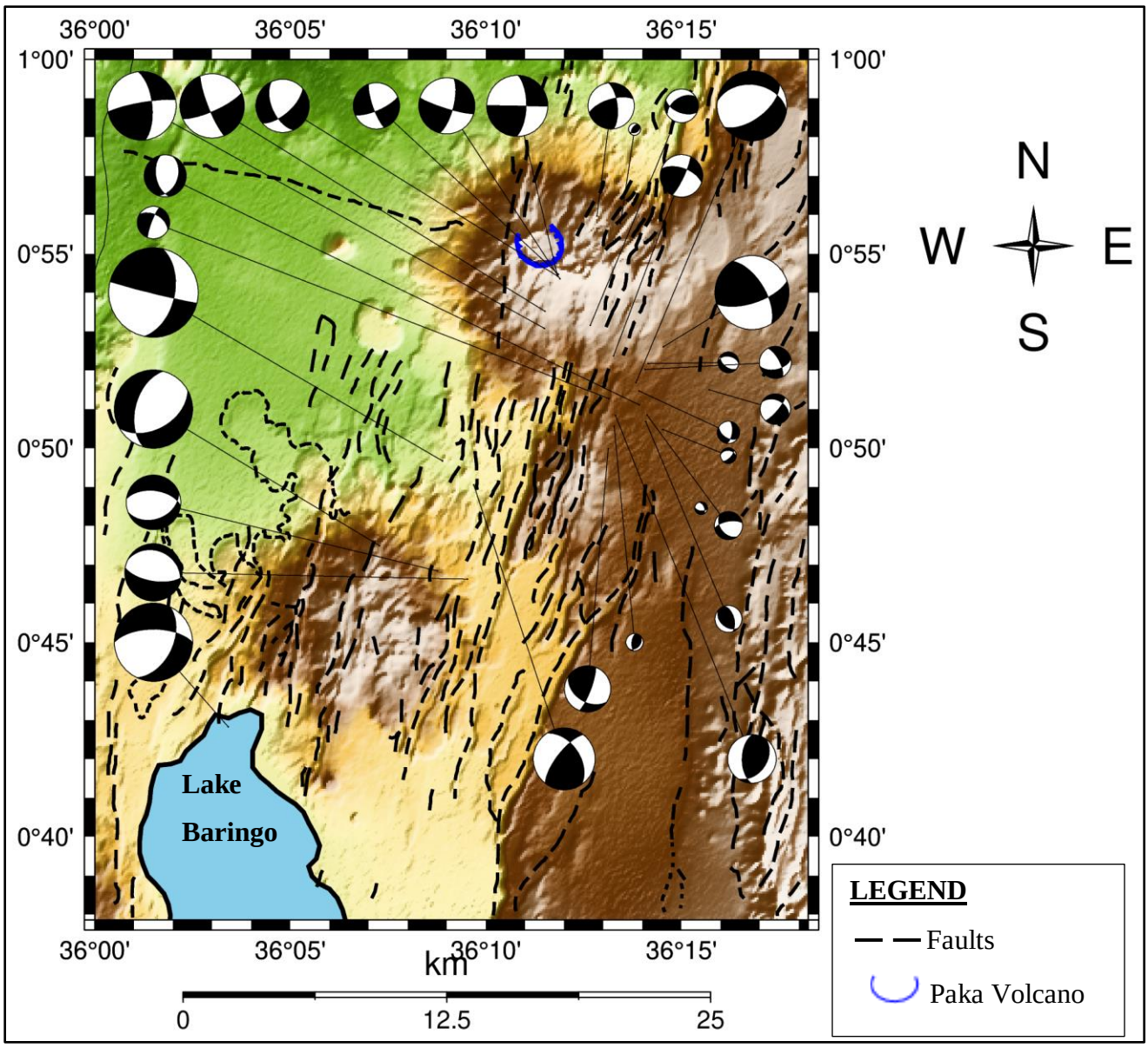

Figure 10: Focal mechanisms for seismic events at the Paka area

The principal stresses; Sigma 1 (S1), Sigma 2 (S2) and Sigma 3 (S3) plunge and azimuth are shown in table 2, these stresses were used to determine the stress regime in the area, the plot of the principal stresses are shown in figure 11.

Table 1: Principal stresses of the Paka area.

S1 plunge/azimuth	S2 plunge/azimuth	S3 plunge/azimuth
55/320	32/114	12/213

The stress inversion on the focal mechanism solutions imply a normal faulting regime in the study area by using the tectonic regime classification method in table 3.

Table 2: Tectonic Regime classification (Zoback, 1992)

P/S1-axis	B/S2-axis	T/S3-axis	Regime	SH- Azimuth
pl > 52		pl < 35	NF	azim. of B-axis
40 < pl < 52		pl < 20	NS	azim. of T-axis + 90°
pl < 40	pl > 45	pl < 20	SS	azim. of T-axis + 90°
pl < 20	pl > 45	pl < 40	SS	azim. of P-axis
pl < 20		40 < pl < 52	TS	azim. of P-axis
pl < 35		pl > 52	TF	azim. of P-axis

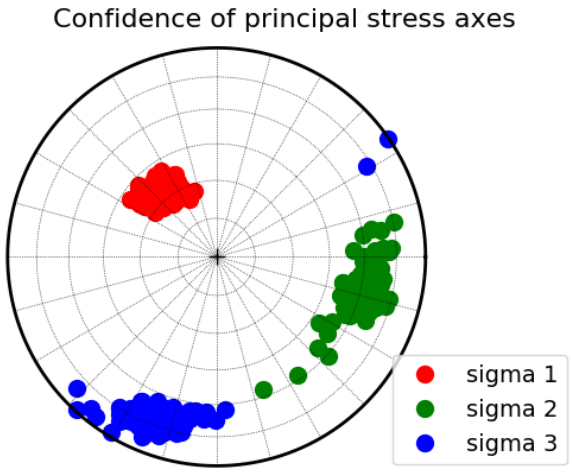

Figure 11: The Principal axes from the stress inversion

The principal fault mechanism solutions (Table 4) determined through the stress inversion and identifed throuth the clustering. The principal faults are the two points on the Mohr circle where the Mohr-Coulomb failure envelope lies on the circle (Vavryčuk, 2014) they also show that the dominant faulting in the area is the normal faulting. The two solutions show that the two faults surfaces strike in the NW-SE direction. The positions of the faults in the Mohr circle are shown in figure 12.

Table 3: Principal fault Mechanism solutions

Principal fault mechanisms	Strike	Dip	Rake
1	108.19	79.54	-122.84
2	310.54	56.49	-50.23

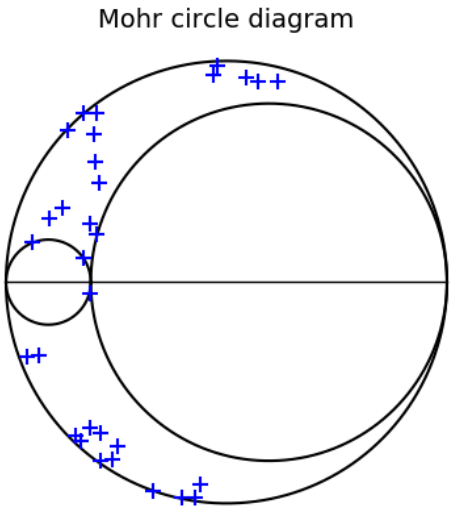

Figure 12: The Mohr Circle diagram showing the positions of the faults.

4.3. Seismic Hydraulic Diffusivity

The seismic hydraulic diffusivity estimates for the earthquake cluster located east of the Paka volcano (figure 13) has values that range from 7.5 $*10^{-2}$ m^2/s to 1.67 m^2/s, figure 14 below shows a map of the diffusivity values for the earthquake cluster located east of the Paka volcano. The average seismic diffusivity value for this cluster is $6.5*10^{-1}m^{2/}s$. The western and south western part of the earthquake cluster shows the high vales of the seismic hydraulic diffusivity. The north eastern and eastern part shows low values of the seismic hydraulic diffusivity.

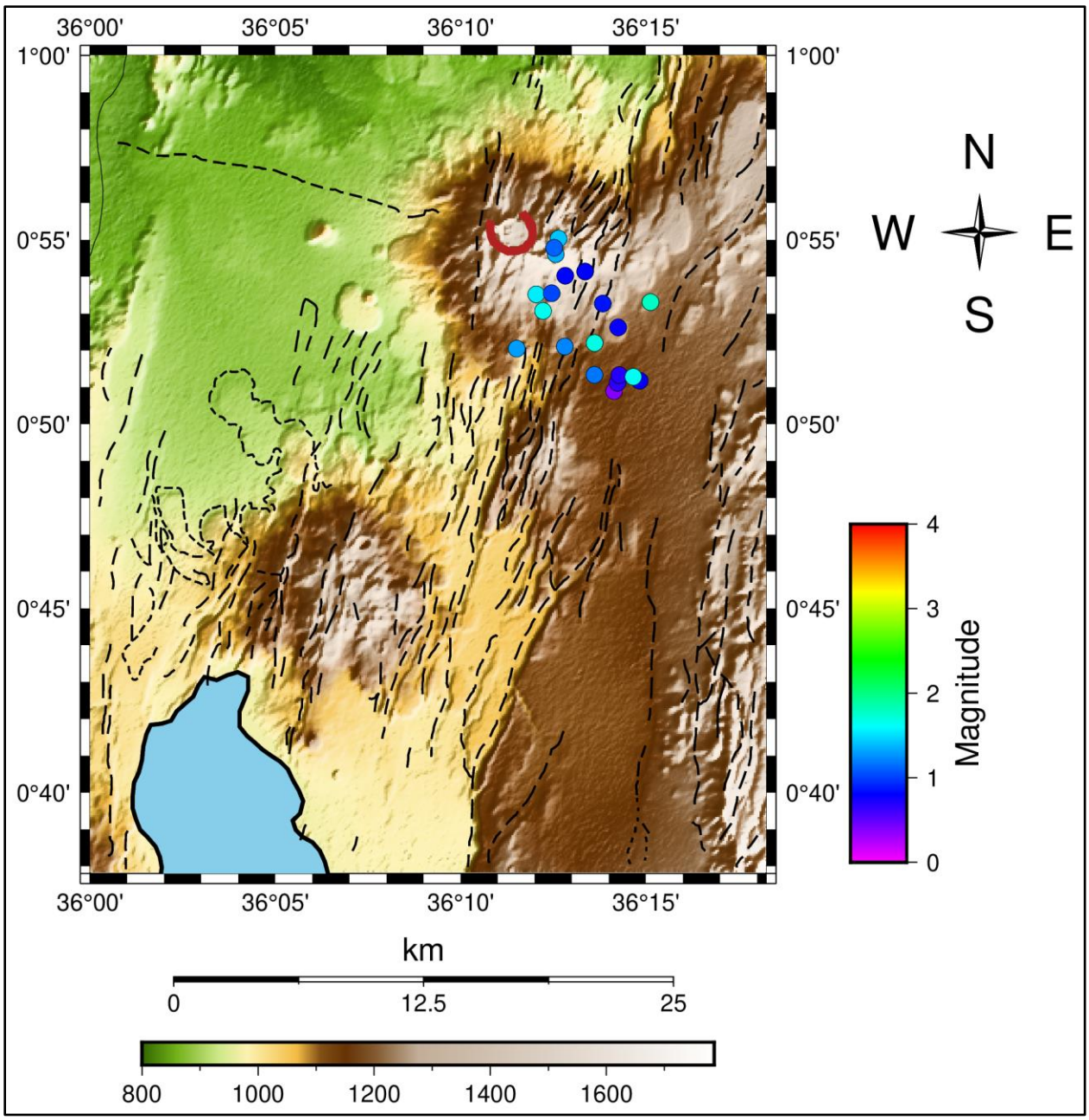

Figure 13: Earthquake cluster location at the Paka Geothermal Prospect

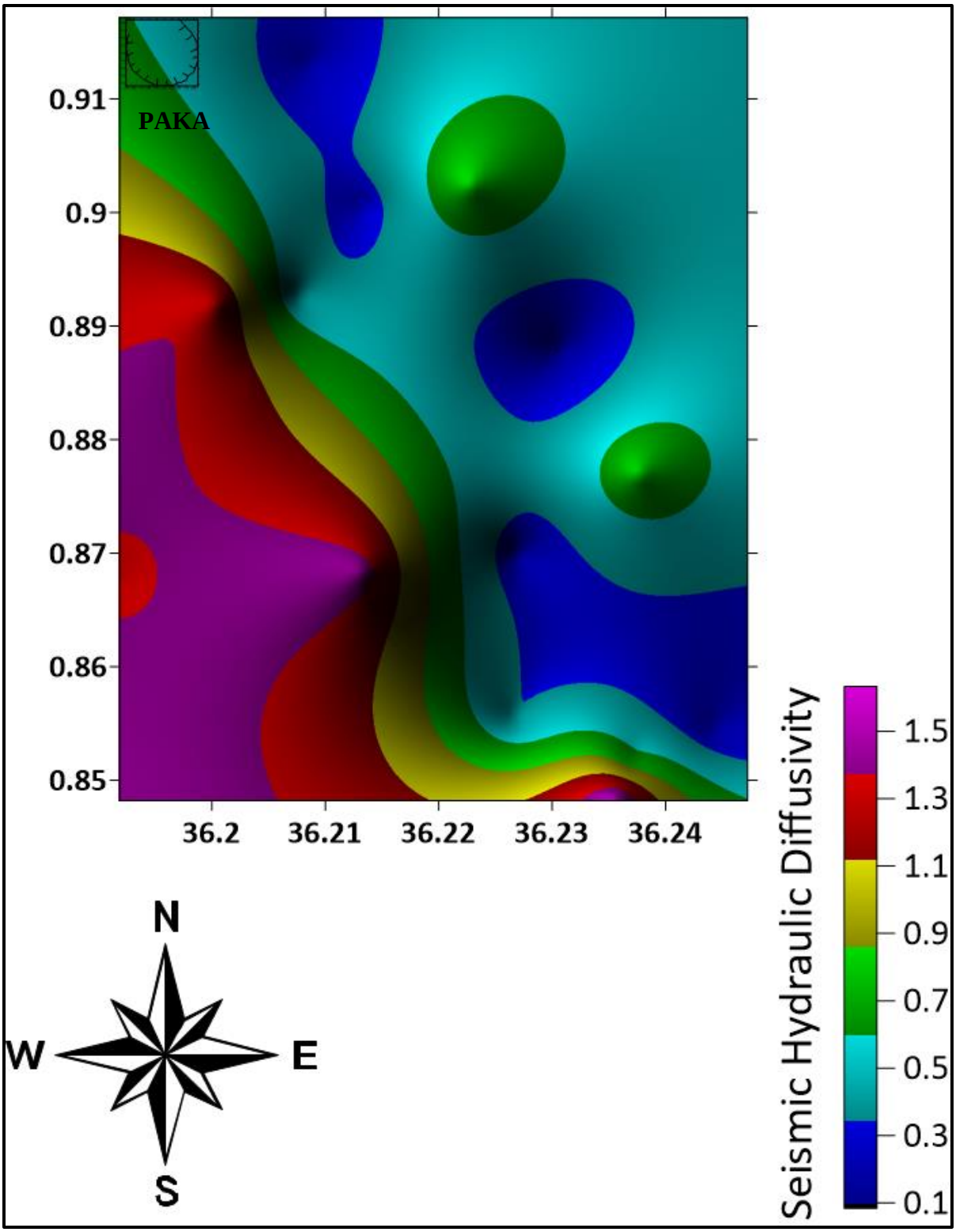

Figure 14: The Seismic Hydraulic Diffusivity map for the earthquake cluster east of Paka volcano

4.4.Discussions

The earthquake events are mainly shallow small magnitude events since they occur along the Kenyan arm of the East African Rift and under a volcano where there is thinning of the crust due to the rifting processes. Teleseismic events were not considered in this study as they were filtered out by the Butterworth filter with corner frequencies of 0.7Hz and 2Hz. The seismically active part of the study area is the area east of the Paka volcano.

The seismic events show linearity to the major rift faults in the area which indicates that the causative faults for those particular events which agree with studies carried out on the Kenyan rift (Kuria et al., 2010; Mulwa & Kimata, 2014; Pointing et al., 1985; Simiyu & Keller, 2000). However, there are few seismic events which do not lie on the major Rift fault zones located beneath the Paka volcano as there are no faults present on the volcano, this area has anomalously low velocities of the S-wave which is due to an active fluid flow that signifies the geothermal potential. The seismic events mainly lie on the faults on the Eastern margins where the geology comprises of the trachytes and tuffs which were extruded towards the end of the second trachytic eruption (Hackman, 1988).

The focal mechanism analysis was done on 31 selected events where 6 or 7 seismic stations were used. From the classification inversion done using the FMC Iterative Joint Inversion software, showed the existence of six fault types namely; normal, normal strike-slip, reverse, reverse strike-slip, strike-slip reverse and strike-slip normal. The dominant fault type is the normal fault type.The inversion of the focal mechanisms for stress analysis show the presence of NW-SE, NE-SW and E-W strike directions on the faults. The Principal stresses show that the tectinic stress regime in the area is the normal faulting regime according to (Zoback, 1992). The principal fault mechanism solutions for the two fault planes that signify the two points in which the Mohr failure evnelope

touches the Mohr circle, also shows that the donimant faulting that occurs at the Paka geothermal system area to be normal faulting, the strike directions for the two planes show a NW-SE strike direction.These solutions show that the distribution of the focal mechanism solutions represents regional tectonic stresses and local magmatic effects on the stresses, this is also the case with the focal mechanisms at the Menengai geothermal area where the orientation in the minimum compressional stress for the normal faults aligns with the regional stresses of the rift system (Patlan et al., 2017). They are also in agreement with the normal, dextral (right lateral), strike slip and sinistral (left lateral) faults in the Magadi area (Kuria et al., 2010).

The main aim of this study is to investigate the role fluids play in initiating seismic activity at the Paka Geothermal Prospect, this has been done by estimating the seismic hydraulic diffusivity which is the hydrologic property that controls the pore pressure in a rock mass in poroelastic deformation. The diffusivity estimates calculated for the earthquake cluster that is located east of the volcano ranges from 7.5 $*10^{-2}$ m^2/s to 1.67 m^2/s with an average seismic diffusivity value for this cluster is $6.5*10^{-1}m^{2/}s$. The western and south western part of the earthquake cluster shows the high vales of the seismic hydraulic diffusivity. The north eastern and eastern part of the earthquake cluster zone shows low values of the seismic hydraulic diffusivity. The area with the high seismic hydraulic diffusivity values lies on the southern flanks of the Paka volcano which extends eastwards in the earthquake cluster zone area, according to (Dunkley et al., 1993; Simiyu, 2010a), these two areas have geothermal activity. The pore pressure diffusion is not controlled by the faults as the distinct boundary between the high diffusive areas and the low diffusive areas runs in an opposite direction to the faults trending in the NNE direction. The crustal hydraulic diffusivity estimates are generally between 10^{-4} m^2/s and 10 m^2/s (Scholz, 2002; Serge A Shapiro et al., 2005), The Vogtland swarms NW Bohemia in 2000 have diffusivity values between 0.3 and

10 m^2/s (Serge A Shapiro et al., 2005), and at the Somma-Vesuvius volcano, Italy have diffusivity values that range from 0.18–0.28 $m^2 s^{-1}$ (Saccorotti et al., 2002). This indicates that the region with high seismic hydraulic diffusivity values have a high pore pressure variation in comparison with the regions with lower seismic hydraulic diffusivity values. This is because pore pressure variation depends on diffusion of fluids in the rock mass which causes reservoir induced seismicity (RIS) as pore pressure diffusion plays a role of triggering seismicity and also causes the ratio between the shear and effective normal stress to exceed the coefficient of friction by the reduction of the effective normal stress in the faults (Baisch & Vörös, 2010; Ferreira et al., 1995; Talwani & Acree, 1985). The fluids flow to the areas with high seismic diffusivity through fractures and faults, which indicate the direction of pore pressure diffusion from areas with low seismic hydraulic diffusivity to areas with high seismic diffusivity leading to pore pressure buildup consequently triggering seismicity (Lupi et al., 2010, 2011). The upflow zone in the Paka geothermal prospect are located in the area that has high seismic hydraulic diffusivities which lies on southern flanks and the southeastern region. They are also in line with the studies on the presence of hydrothermic minerals the clay minerals such as kaolinite that occur in the fault zones in the geothermal prospect (Achieng et al., 2017)and the fumarolic condensates that also occur within the geothermal prospect in Paka (Mulusa, 2015). The seismic events that lie in the areas with high seismic hydraulic diffusivity are caused by pore pressure diffusion through the faults and fractures rather than the bulk of the rock (Talwani et al., 2007) which are the high permeability zones that act as conduits of convective heat transfer.

The seismic events that occur as a result of volcano-tectonic movements are all the other relocated events that did not lie on the earthquake cluster zone. This is because the earthquakes that occur as a result of the fluid flow exhibit swarm like characteristics and occur in clusters. These events

caused by the volcano-tectonic movements show linearity in the faults which indicates that they result from the rifting process. The area where the earthquake cluster is located has a low velocity of the S-wave which indicates the existence of fluid movements, this was also used to select the area for further analysis on the seismic activity.

CHAPTER 5. CONCLUSIONS AND RECOMMENDATIONS

5.1. Conclusions

The seismic events are generally shallow small magnitude events as they occur along the Kenyan arm of the East African Rift and under a volcano where there is thinning of the crust due to the rifting and volcanic processes in the geothermal prospect area. The events show linearity with the major rift faults which are the causative faults of those particular events implying that the rifting process plays a role in initiating the earthquakes.

The focal mechanism solutions show that although the faulting of the Kenyan Rift valley is predominantly normal faulting, the faulting at the Paka geothermal prospect has; normal, normal strike-slip, reverse, reverse strike-slip, strike-slip reverse and strike-slip normal. The dominant fault type is the normal fault type. The strike directions from the inversion of the focal mechanism solutions are NW-SE, NE-SW and E-W strike directions on the faults. The Principal stresses show that the tectinic stress regime in the area is the normal faulting regime. The principal fault mechanism solutions for the two fault planes also shows that the donimant faulting that occurs at the Paka geothermal system area to be normal faulting, the strike directions for the two planes show a NW-SE strike direction.These solutions show that the distribution of the focal mechanism solutions represents regional tectonic stresses and local magmatic effects on the stresses.

The seismic events found in the areas with high seismic hydraulic diffusivity in the Paka geothermal prospect are interpreted as to be caused by fluid movement this is because this zone of the earthquake clusters also has low velocities of the S-wave indicating the presence of fluids. The volcano-tectonic events do not have the characteristic of earthquake clustering and show linearity to the causative faults. The study also agrees with Simiyu's and Dunkley's study on the geothermal

active zones where the southern flanks of the Paka volcano has high seismic diffusivities of up to 1.67 m^2/s which lies on the southern flanks and is also an active geothermal area. The faults and fractures where the pore pressure diffusion takes place are the zones of high permeability that act as conduits of convective heat transfer. The upflow zones in the study area lie in the regions that have high seismic hydraulic diffusivities. Pore pressure is not the only triggering mechanism, as all earthquakes do not lie in the cluster and the earth is dynamic.

5.2. Recommendations

The region on the southern flanks of Paka volcano that extends eastwards that lies in the earthquake cluster area is the most suitable target for drilling high fluid producing wells as there is high pore pressure diffusion within the reservoir.

Similar studies should be carried out in the geothermal prospects within the Kenyan Rift valley that have not started production and fluid-reinjection as the seismic hydraulic diffusivity estimation is an effective tool in determining the pore pressure diffusion and therefore understanding the fluid rock interaction.

REFERENCES

Achieng, J., Mutua, J., Mibei, G., Olaka, L., & Waswa, A. K. (2017). Mapping of Hydrothermal Minerals Related to Geothermal Activities Using Remote Sensing and GIS : Case Study of Paka Volcano in Kenyan Rift Valley. *International Journal of Geosciences*, *8*, 711–725. https://doi.org/10.4236/ijg.2017.85039

Álvarez-Gómez, J. A. (2019). FMC—Earthquake focal mechanisms data management, cluster and classification. *SoftwareX*, *9*, 299–307. https://doi.org/10.1016/j.softx.2019.03.008

Andreassen, K. A., & Fabricius, I. L. (2010). Biot Critical Frequency Applied As Common Friction Factor For Chalk With Different Pore Fluids And Temperatures. *44th U.S. Rock Mechanics Symposium and 5th U.S.-Canada Rock Mechanics Symposium*, 10. https://doi.org/

Aochi, H., Poisson, B., Toussaint, R., Rachez, X., & Schmittbuhl, J. (2013). Self-induced seismicity due to fluid circulation along faults. *Geophysical Journal International*, *196*, 611. https://doi.org/10.1093/gji/ggt356

Audin, L., Avouac, J.-P., Flouzat, M., & Plantet, J.-L. (2002). Fluid-driven seismicity in a stable tectonic context: The Remiremont fault zone, Vosges, France. *Geophysical Research Letters*, *29*(0). https://doi.org/10.1029/2001GL012988

Baisch, S., & Vörös, R. (2010). Reservoir Induced Seismicity : Where , When , Why and How Strong ? *Proceedings World Geothermal Congress 2010*, *April*.

Becker, J., & Weber, B. (2015). *SeisComP3 -Introduction to scconfig* (pp. 1–35).

Boit, M. A. (1962). Mechanics of Deformation and Acoustic Propagation in Porous Media. *Journal of Applied Physiscs*, *33*(4), 1482–1498.

https://doi.org/10.1001/archotol.1995.01890060005001

Bondár, I., Myers, S. C., Engdahl, E. R., & Bergman, E. A. (2004). Epicentre accuracy based on seismic network criteria. *Geophysical Journal International*, *156*(3), 483–496. https://doi.org/10.1111/j.1365-246X.2004.02070.x

Bourouis, S., & Cornet, F. H. (2009). Microseismic activity and fluid fault interactions : some results from the Corinth Rift Laboratory (CRL), Greece. *Geophys. J. Int.*, *178*, 561–580. https://doi.org/10.1111/j.1365-246X.2009.04148.x

Brauer, K., Kampf, H., Strauch, G., & Weise, S. M. (2003). Isotopic evidence (3 He / 4 He , seismicity C CO 2) of fluid-triggered intraplate. *JOURNAL OF GEOPHYSICAL RESEARCH*, *108*(B2). https://doi.org/10.1029/2002JB002077

Brehme, M., Blöcher, G., Cacace, M., Deon, F., Moeck, I., Wiegand, B., Kamah, Y., Regenspurg, S., Zimmermann, G., Sauter, M., & Huenges, E. (2016). Characterizing permeability structures in geothermal reservoirs – A case study in Lahendong. *PROCEEDINGS, 41st Workshop on Geothermal Reservoir Engineering Stanford University, Stanford, California*, 22–24.

Chen, X., Shearer, P. M., & Abercrombie, R. E. (2012). Spatial migration of earthquakes within seismic clusters in Southern California: Evidence for fluid diffusion. *Journal of Geophysical Research*, *117*(BO4301). https://doi.org/10.1029/2011JB008973

Chouliaras, G., Kassaras, I., Kapetanidis, V., Petrou, P., & Drakatos, G. (2015). Seismotectonic analysis of the 2013 seismic sequence at the western Corinth Rift. *Journal of Geodynamics*, *90*, 42–57. https://doi.org/10.1016/j.jog.2015.07.001

Cornet, F. H. (2016). Geomechanics for Energy and the Environment Seismic and aseismic motions generated by fluid injections. *Geomechanics for Energy and the Environment*, *5*, 42–54. https://doi.org/10.1016/j.gete.2015.12.003

Corti, G., Cioni, R., Franceschini, Z., Sani, F., Scaillet, S., Molin, P., Isola, I., Mazzarini, F., Brune, S., Keir, D., Erbello, A., Muluneh, A., Illsley-kemp, F., & Glerum, A. (2019). Aborted propagation of the Ethiopian rift caused by linkage with the Kenyan rift. *Nature Communications*, *10*(1309), 1–11. https://doi.org/10.1038/s41467-019-09335-2

Cronin, V. (2010). Focal_mechanism_primer.pdf. *A Primer on Focal Mechanism Solutions for Geologists*, 14.

Dinske, C. (2010). Interpretation of Fluid-Induced Seismicity at Geothermal and Hydrocarbon Reservoirs of Basel and Cotton Valley. In *Fachbereich Geowissenschaften*. Freien Universität Berlin.

Doan, M. L., Brodsky, E. E., Kano, Y., & Ma, K. F. (2006). In situ measurement of the hydraulic diffusivity of the active Chelunepu Fault, Taiwan. *Geophysical Research Letters*, *33*(L16317). https://doi.org/10.1029/2006GL026889

Doser, D. I. (1994). Deep crustal earthquakes associated with continental rifts. *Tectonophysics*, *229*, 123–131.

Dunkley, P. N., Smith, M., Allen, D. J., & Darling, W. G. (1993). *The geothermal activity and geology of the northern sector of the Kenya Rift Valley*.

Ebinger, C. J., Muirhead, J. D., Roecker, C., Tiberi, C., Muzuka, A., Ferdinand, R., Mulibo, G., & Kianji, G. (2015). Rift initiation with volatiles and magma. *EGU General Assembly*,

17(EGU2015-3698).

Ebinger, C., Olivia, S. J., Peterson, K. E., Chindandali, P. R. N., Illsley-kemp, F., Shillington, D. J., Accardo, N. J., Gallacher, R. J., Gaherty, J. B., & Nyblade, A. A. (2019). Kinematics of Active Deformation in the Malawi Rift and Rungwe Volcanic Province, Africa. *Geochemistry, Geophysics, Geosystems*, *20*(8), 3928–3951. https://doi.org/10.1029/2019GC008354

Ferreira, J. M., De Oliveira, R. T., Assumpaco, M., Moreira, J. A. M., Pearce, R. G., & Takeya, M. K. (1995). Correlation of Seismicity and Water Level in the Example from Northeast Brazil. *Bulletin of the Seismological Society of America, 85*(5), 1483–1489.

Fonseca, J. F. B. D., Chamussa, J., Domingues, A., Helffrich, G., Antunes, E., van Aswegen, G., Pinto, L. V., Custodio, S., & Manhica, V. J. (2014). MOZART: A Seismological Investigation of the East African Rift in Central Mozambique. *Seismological Research Letters*, *85*(1), 108–116. https://doi.org/10.1785/0220130082

Foulger, G. (1982). Geothermal exploration and reservoir monitoring using earthquakes and the passive seismic method. *Geothermics*, *11*(4), 259–268. https://doi.org/10.1016/0375-6505(82)90032-3

Friese, & Andrea. (2015). *InSAR, structural analyses and dating of Paka volcanic products, Northern Kenya Rift*.

Hackman, B. D. (1988). *Geology of the Baringo-Laikipia area. R*. Derry and Sons Limited, Nottingham.

Hu, J. (n.d.). *GMT EX04 : Focal Mechanism*.

Hutchison, W., Mather, T. A., Pyle, D. M., Biggs, J., & Yirgu, G. (2015). Structural controls on fluid pathways in an active rift system: A case study of the Aluto volcanic complex. *Geosphere*, *11*(3), 542–562. https://doi.org/10.1130/GES01119.1

Jasim, A., Whitaker, F. F., & Rust, A. C. (2015). Impact of channelized flow on temperature distribution and fluid flow in restless calderas: Insight from Campi Flegrei caldera, Italy. *Journal of Volcanology and Geothermal Research*, *303*, 157–174. https://doi.org/10.1016/j.jvolgeores.2015.07.029

Johann, L., Dinske, C., & Shapiro, S. A. (2016). Scaling of seismicity induced by nonlinear fluid-rock interaction after an injection stop. *Journal of Geophysical Research: Solid Earth*, *121*(11). https://doi.org/10.1002/2016JB012949

Kamei, R., Nakata, N., & Lumley, D. (2015). Introduction to microseismic source mechanisms. *Leading Edge*, *34*(8), 876–880. https://doi.org/10.1190/tle34080876.1

Kangogo, D., Kamau, P., Kiama, J., Mukiri, R., & Nguuri, T. (2018). The Crustal Structure of Northern Kenya Rift : Results from micro Earthquakes Data. *The Crustal Structure of Northern Kenya Rift: Results from Micro Earthquakes Data*, *November*.

Kebede, F., & Kulhánek, O. (1991). Recent seismicity of the East African Rift system. *Physics of the Earth and Planetary Interiors*, *68*, 259–273.

Khalil, A. R., & Al-Arifi, N. S. (2018). Focal mechanisms overview. *Earth Science Informatics*, *12*(3), 381–388. https://doi.org/10.1007/s12145-018-0367-1

King, G. C. P., Ouyang, Z. X., Papadimitriou, P., Deschamps, A., Gagnepain, J., Houseman, G., Jackson, J. A., Soufleris, C., & Virieux, J. (1985). The evolution of the Gulf of Corinth

(Greece): an aftershock study of the 1981 earthquakes. *Geophys. J. R. Astr. Soc*, *80*, 677–693.

Kuria, Z. N., Woldai, T., Meer, F. D. van der, & Barongo, J. O. (2010). Active fault segments as potential earthquake sources: Inferences from integrated geophysical mapping of the Magadi fault system, southern Kenya Rift. *Journal of African Earth Sciences*, *57*, 345–359. https://doi.org/10.1016/j.jafrearsci.2009.11.004

Lupi, M., Geiger, S., & Graham, C. M. (2010). Hydrothermal fluid flow within a tectonically active rift-ridge transform junction: Tj??rnes Fracture Zone, Iceland. *Journal of Geophysical Research: Solid Earth*. https://doi.org/10.1029/2009JB006640

Lupi, M., Geiger, S., & Graham, C. M. (2011). Numerical simulations of seismicity-induced fluid flow in the Tjrnes Fracture Zone, Iceland. *Journal of Geophysical Research*, *116*(B07101). https://doi.org/10.1029/2010JB007732

Mackenzie, G. D., Thybo, H., & Maguire, P. K. H. (2005). Crustal velocity structure across the Main Ethiopian Rift: Results from two-dimensional wide-angle seismic modelling. *Geophysical Journal International*, *162*(3), 994–1006. https://doi.org/10.1111/j.1365-246X.2005.02710.x

Mbia, P. K. (2014). *Sub-Surface Geology, Petrology and Hydrothermal Alteration of Menengai Geothermal Field, Kenya*. University of Iceland.

Mcnutt, S. R. (2005). VOLCANIC SEISMOLOGY. *Annual Review of Earth and Planetary Sciences*, *33*(1), 461–491. https://doi.org/10.1146/annurev.earth.33.092203.122459

Mekkawi, M., Schnegg, P.-A., Arafa-Hamed, T., & Elathy, E. (2005). Electrical structure of the tectonically active Kalabsha Fault ,. *Earth and Planetary Science Letters*, *240*, 764–773.

https://doi.org/10.1016/j.epsl.2005.09.035

Mibei, G. (2012). *Geology and Hydrothermal Alteration of Menengai Geothermal Field. Case Study: Wells MW-04 AND MW-05*.

Mibei, G., Harðarson, B. S., Franzson, H., Bali, E., Geirsson, H., & Guðfinnsson, G. H. (2020). Eruptive history and volcano-tectonic evolution of Paka volcanic complex in the northern Kenya rift: Insights into the geothermal heat source. *Journal of African Earth Sciences*. https://doi.org/10.1016/j.jafrearsci.2020.103951

Michelet, S., & Toksoz, M. N. (2007). Fracture mapping in the Soultz-sous-For its geothermal field using microearthquake locations. *Journal of Geophysical Research: Solid Earth*, *112*(B07315). https://doi.org/10.1029/2006JB004442

Mulusa, G. (2015). Geochemical Study of Fumarolic Condensates from Paka Volcano, Kenya. *Proceedings World Geothermal Congress 2015*, *April*, 19–25.

Mulwa, J. K., & Kimata, F. (2014). Tectonic structures across the East African Rift based on the source parameters of the 20 May 1990 M7.2 Sudan earthquake. *Natural Hazards*, *73*(2), 493–506. https://doi.org/10.1007/s11069-014-1082-y

Mutonga, M. (2013). The Geology of Paka Volcano, and its Implication on Geothermal. *GRC Transactions*, *37*.

Mutonga, M. (2016). *The geology of Paka volcano , and its implication on geothermal The Geology of Paka Volcano , and its Implication on Geothermal*. *January 2013*.

Nelson, S. A. (2013). *Earthquakes : Causes and Measurements*.

Njue, L. M. (2015). Geological Model of Korosi Geothermal Prospect, Kenya. *Proceedings World*

Geothermal Congress, 19–25.

Noir, J., Jacques, E., Békri, S., Adler, P. M., Tapponnier, P., & King, G. C. P. (1997). Fluid flow triggered migration of events in the 1989 Dobi earthquake sequence of Central Afar. *Geophysical Research Letters*, *24*(18), 2335–2338. https://doi.org/10.1029/97GL02182

Oliva, S. J., Ebinger, C. J., Wauthier, C., Muirhead, J. D., Roecker, S. W., & Rivalta, E. (2019). *Insights into fault - magma interactions in an early - stage continental rift from source mechanisms and correlated volcano - tectonic earthquakes*. https://doi.org/10.1029/2018GL080866

Oliva, S. J., Ebinger, C. J., Wauthier, C., Muirhead, J. D., Roecker, S. W., Rivalta, E., & Heimann, S. (2019). Insights Into Fault-Magma Interactions in an Early-Stage Continental Rift From Source Mechanisms and Correlated Volcano-Tectonic Earthquakes. *Geophysical Research Letters*, *46*(4), 2065–2074. https://doi.org/10.1029/2018GL080866

Omenda, P. A. (2008). Status of Geothermal Exploration in Kenya and Future Plans for Its Development. In *Short Course III on Exploration for Geothermal Resources,*.

Omenda, P., Simiyu, S., & Muchemi, G. (2014). Geothermal Country Update Report for Kenya: 2014. *ARGeo-C5*, 29–31.

Parotidis, M., Rothert, E., & Shapiro, S. A. (2003). Pore-pressure diffusion : A possible triggering mechanism for the earthquake swarms 2000 in Vogtland /NW-Bohemia , central Europe. *Geophysical Research Letters*, *30*(20), 10–13. https://doi.org/10.1029/2003GL018110

Parotidis, M., Shapiro, S. A., & Rothert, E. (2005). Evidence for triggering of the Vogtland swarms 2000 by pore pressure diffusion. *Journal of Geophysical Research*, *110*(B05S10), 1–12.

https://doi.org/10.1029/2004JB003267

Patlan, E., Velasco, A. A., Wamalwa, A., & Kaip, G. (2017). Seismic Zone at East Africa Rift: Insights into the Geothermal Potential. *42nd Workshop on Geothermal Reservoir Engineering*, 13–15.

Pointing, A. ., Maguire, P. K. H., Khan, M. A., Francis, D. J., Swain, C. J., Shah, E. R., & Griffiths, D. H. (1985). Seismicity of the northern valley part of the kenya rift. *Journal of Geodynamics*, *37*(3), 23–37.

Prodehl, C., Ritter, J. R. R., Mechie, J., Keller, G. R., Khan, M. A., Jacob, B., Fuchs, K., Nyambok, I. O., Obel, J. D., & Riaroh, D. (1997). The KRISP 94 lithospheric investigation of southern Kenya experiments and their main results the. *Tectonophysics*, *278*, 121–147.

Raziperchikolaee, S., Alvarado, V., & Yin, S. (2014). Microscale modeling of fluid flow-geomechanics-seismicity: Relationship between permeability and seismic source response in deformed rock joints. *Journal of Geophysical Research, Solid Earth*. https://doi.org/10.1002/2013JB010758

REF TEK Utilities Users Guide (p. 156). (2006). Refraction technology, Inc. http://reftek.com

Riaroh, D., & Okoth, W. (1994). The geothermal fields of the Kenya rift. *Tectonophysics*, *236*, 117–130. https://doi.org/10.1016/0040-1951(94)90172-4

Riedl, S., Melnick, D., Mibei, G. K., Njue, L., & Strecker, M. R. (2019). Continental rifting at magmatic centres: Structural implications from the Late Quaternary Menengai Caldera, Central Kenya Rift. *Journal of the Geological Society*, *177*(1), 153–169. https://doi.org/10.1144/jgs2019-021

Robertson, E. A. M., Biggs, J., Cashman, K. V., Floyd, M. A., & Vye-Brown, C. (2015). Influence of regional tectonics and pre-existing structures on the formation of elliptical calderas in the Kenyan Rift. *Geological Society, London, Special Publications*, *420*. https://doi.org/10.1144/SP420.12

Roecker, S., Ebinger, C., Tiberi, C., Mulibo, G., Ferdinand-Wambura, R., Mtelela, K., Kianji, G., Muzuka, A., Gautier, S., Albaric, J., & Peyrat, S. (2017). Subsurface images of the Eastern Rift, Africa, from the joint inversion of body waves, surface waves and gravity: Investigating the role of fluids in early-stage continental rifting. *Geophysical Journal International*, *210*(2), 931–950. https://doi.org/10.1093/gji/ggx220

Saccorotti, G., Ventura, G., Vilardo, G., & Vilardo, G. (2002). Seismic swarms related to diffusive processes: The case of Somma-Vesuvius volcano, Italy. *Geophysics*, *67*(1), 199–203. https://doi.org/10.1190/1.1451551

Saul, J., Heinloo, A., & Becker, J. (2015). *What is SeisComP ?* (pp. 1–3).

Scholz, C. H. (2002). Scholz, C. H. 2002. The Mechanics of Earthquakes and Faulting, 2nd edition. In *Cambridge University Press.* https://doi.org/10.1017/S0016756803227564

Schönholzer, S. (2009). Assessing the solution quality of the earthquake location problem. In *ETH Zurich*. ETH Zurich.

Schuite, J., Longuevergne, L., Bour, O., Burbey, T. J., Boudin, F., Lavenant, N., & Davy, P. (2017). Understanding the Hydromechanical Behavior of a Fault Zone From Transient Surface Tilt and Fluid Pressure Observations at Hourly Time Scales. *Water Resources Research*, *53*(12), 10558–10582. https://doi.org/10.1002/2017WR020588

Scuderi, M. M., & Collettini, C. (2016). The role of fluid pressure in induced vs. triggered seismicity: insights from rock deformation experiments on carbonates. *Scientific Reports*, *6*(1), 24852. https://doi.org/10.1038/srep24852

SeisComP3 Seattle documentation (Seattle). (2013). GFZ Postdam, gempa GmbH. https://www.seiscomp3.org/doc/seattle/2013.046/index.html

Shapiro, S. A., Huenges, E., & Borm, G. (1997). Estimating the crust permeability from fluid-injection-induced seismic emission at the KTB site. *Geophysical Journal International*, *131*(2), 5–8. https://doi.org/10.1111/j.1365-246X.1997.tb01215.x

Shapiro, S. A., Patzig, R., Rothert, E., & Rindschwentner, J. (2003). Triggering of Seismicity by Pore-pressure Perturbations: Permeability-related Signatures of the Phenomenon. *Pure and Applied Geophysics*, *160*, 1051–1066. https://doi.org/10.1007/PL00012560

Shapiro, S A, & Dinske, C. (2009). Fluid-induced seismicity : Pressure diffusion and hydraulic fracturing. *Geophysical Prospecting*, *57*, 301–310. https://doi.org/10.1111/j.1365-2478.2008.00770.x

Shapiro, Serge A. (2000). An inversion for fluid transport properties of three-dimensionally heterogeneous rocks using induced microseismicity. *Geophys. J. Int*, *143*, 931–936.

Shapiro, Serge A, Rentsch, S., & Rothert, E. (2005). Characterization of hydraulic properties of rocks using probability of fluid-induced microearthquakes. *GEOPHYSICS*, *70*(2), 27–33.

Shapiro, Serge A, Rothert, E., Rath, V., & Rindschwentner, J. (2002). Characterization of fluid transport properties of reservoirs using induced microseismicity. *GEOPHYSICS*, *67*(1), 212–220.

Sigmundsson, F., Einarsson, P., Rognvaldsson, T., Foulger, G. R., Hodgkinson, K. M., & Thorbergsson, G. (1997). The 1994-1995 seismicity and deformation at the Hengill triple. *Journal of Geophysical Research*, *102*(July 1994), 15151–16161. https://doi.org/10.1029/97JB00892

Šílený, J., Jechumtálová, Z., & Dorbath, C. (2014). Small Scale Earthquake Mechanisms Induced by Fluid Injection at the Enhanced Geothermal System Reservoir Soultz (Alsace) in 2003 using Alternative Source Models. *Pure and Applied Geophysics*, *171*(10). https://doi.org/10.1007/s00024-013-0750-2

Simiyu, S. M. (1999). Induced micro-seismicity during well discharge : *Geothermics*, *28*, 785–802.

Simiyu, S. M. (2000). Geothermal reservoir characterization: Application of microseismicity and seismic wave properties at Olkaria, Kenya rift. *Journal of Geophysical Research*, *105795*(10), 779–13. https://doi.org/10.1029/1999JB900401

Simiyu, S. M. (2010a). Status of Geothermal Exploration in Kenya and Future Plans for Its Development. In *World Geothermal Congress 2010* (Issue April).

Simiyu, S. M. (2014). *Application of Micro-Seismic Methods to Geothermal Exploration: Examples from the Kenya Rift* (pp. 1–27).

Simiyu, S. M. (2010b). Status of Geothermal Exploration in Kenya and Future Plans for Its Development. *World Geothermal Congress 2010*, 25–29.

Simiyu, S. M., & Keller, G. R. (2000). Seismic monitoring of the Olkaria Geothermal area, Kenya Rift valley. *Journal of Volcanology and Geothermal Research*, *95*, 197–208.

www.elsevier.comrlocaterjvolgeores

Sira, C., Schlupp, A., Schaming, M., Chesnais, C., Cornou, C., Dechamp, A., Delavaud, E., & MaufroyE. (2014). *RapportSismologiqueBCSF-Sei07Avril2014-Barcelonnette-BD.pdf*.

Skoumal, R. J., Brudzinski, M. R., Currie, B. S., & Levy, J. (2014). Optimizing multi-station earthquake template matching through re-examination of the Youngstown, Ohio, sequence. *Earth and Planetary Science Letters*, *405*, 274–280. https://doi.org/10.1016/j.epsl.2014.08.033

Spicak, A., & Horalek, J. (2001). Possible role of fluids in the process of earthquake swarm generation in the West Bohemia / Vogtland seismoactive region. *Tectonophysics*, *336*, 151–161.

Talwani, P., & Acree, S. (1985). Pore Pressure Diffusion and the Mechanism of Reservoir-Induced Seismicity. *PAGEOPH*, *122*, 947–965. https://doi.org/10.1007/978-3-0348-6245-5_14

Talwani, P., Chen, L., & Gahalaut, K. (2007). Seismogenic permeability , k s. *JOURNAL OF GEOPHYSICAL RESEARCH*, *112*(B07309), 1–18. https://doi.org/10.1029/2006JB004665

The Generic Mapping Tools Documentation. (2019). http://gmt.soest.hawaii.edu/projects/gmt/wiki/Documentation

Tongue, J., Maguire, P., & Burton, P. (1994). An earthquake study in the Lake Baringo basin of the central Kenya Rift. *Tectonophysics*, *236*, 151–164. https://doi.org/10.1016/0040-1951(94)90174-0

Tumwikirize, I. (2014). Passive Seismic Network: A Diagnostic Tool to Discover Geothermal Activity Isaiah Tumwikirize Geological Survey and Mines Ministry of Energy and Mineral

Development. *5th African Rift Geothermal Conference*, 29–31.

Vavryčuk, V. (2014). Iterative joint inversion for stress and fault orientations from focal mechanisms. *Geophysical Journal International*, *199*(1), 69–77. https://doi.org/10.1093/gji/ggu224

Vavryčuk, V. (2015). Earthquake Mechanisms and Stress Field. In *Encyclopedia of Earthquake Engineering*. https://doi.org/10.1007/978-3-642-36197-5_295-1

Wadge, G., Biggs, J., Lloyd, R., & Kendall, J. M. (2016). Historical volcanism and the state of stress in the east African rift system. *Frontiers in Earth Science*, *4*. https://doi.org/10.3389/feart.2016.00086

Walters, R., & Wijk, K. van. (2009). Seismicity Associated with Geothermal Systems. *ResearchGate*.

Wang, H. F. (2000). Theory of Linear Poroelasticity with Applications to Geomechanics and Hydrogeology. In *Princeton University Press*. https://doi.org/10.1515/9781400885688

Yagi, Y. (n.d.-a). *Earthquake Focal Mechanism*. https://iisee.kenken.go.jp/lna/download.php?f=2015032092f656cd.pdf&n=S-250-2013_Moment_Tensor_Analysis1(Yagi).pdf&cid=S0-250-2013

Yagi, Y. (n.d.-b). *Seismic Source Mechanism*. http://www.geol.tsukuba.ac.jp/~yagi-y/text/Source_meca_v0.7.pdf

Yamashita, T., & Tsutsumi, A. (2018). Involvement of Fluids in Earthquake Ruptures. In *Involvement of Fluids in Earthquake Ruptures*. Springer Japan KK. https://doi.org/10.1007/978-4-431-56562-8

Zahirovic, S. (2016). *Data Processing and Plotting Using Generic Mapping Tools (GMT)*.

Zoback, M. L. (1992). First-and second-order patterns of stress in the lithosphere: the World Stress Map Project. *Journal of Geophysical Research*, *97*(B8). https://doi.org/10.1029/92jb00132

APPENDICES

Appendix 1: Commands used in the location in Seiscomp3

To scart and pick the changes in amplitude;

scart -dvsE -t '2013-01-01 00:00:00~2016-12-31 23:59:59' | scautopick -d mysql://seismics:seismics@localhost/seiscomp3 --playback --ep -I - > picks.xml.

To locate events;

scautoloc --ep picks.xml -d mysql://seismics:seismics@localhost/seiscomp3 --playback --xxl-enable=1 --debug > origins.xml

To calculate the amplitudes;

scamp –d mysql://seismics:seismics@localhost/seiscomp3 -I sdsarchive: ///home/seismics/seiscomp3/var/lib/archive --ep origins2016.xml --debug > origins-with-amps.xml

To calculate magnitudes;

scmag -d mysql://seismics:seismics@localhost/seiscomp3 --ep origins-with-amps.xml --debug > origins-with-mags.xml

To determine events;

scevent --ep origins-with-mags.xml --debug > eventsf.xml.

To load events to the database;

scdb -i eventsf.xml -d mysql://seismics:seismics@localhost/seiscomp3

To relocate events;

scrtdd --reloc-profile myprofile --verbosity=3 --console=1 -d mysql://seismics:seismics@localhost/seiscomp3